CHAPTER 5

CHAPTER 5

Metamorphic evolution

The high-grade Central Gneissic Belt situated at the central part of the province is composed of felsic gneiss, migmatitic hornblende gneiss, charnockite gneiss, enclaves of mafic granulite and amphibolite and also basic and felsic intrusives. The Central Gneissic Belt is flanked on north and south by low-grade Northern Supracrustal Belt and the Southern Supracrustal Belt, composed of mainly of quartzite and mica schist, with minor proportion of meta-conglomerate, metachert, metabasic rocks and BIF components. The felsic and migmatitic hornblende gneisses of the gneissic belt have undergone amphibolite facies metamorphism, whereas the charnockite gneiss and the mafic granulite enclave suite preserve the evidences of granulite facies metamorphism. The Southern and Northern Supracrustal Belts have suffered a lower grade of metamorphism, maximum attaining up to greenschist facies as evident from the mineral assemblages.

5.1 Methodology

To understand the metamorphic evolution of the Rengali Province, petrographic study of the high- and low-grade rocks were carried out (Table 5.1). Mineral chemical characterization of the high-grade rocks was done to understand the chemical attributes of metamorphic processes and estimation of pressure and temperature conditions of different stages of metamorphism. For petrographic study, both polarized light microscopy and scanning electron microscopy were used. In the former case, a Nikon Eclipse LV100 polarizing microscope was used which was fitted with a digital camera and a computer with Nikon image processing software. For scanning electron microscopy, the Tescan Vega LSU scanning electron microscope with Oxford Instruments EDAX facility was used. Back Scatter

Electron imaging was done for all critical microdomains to understand the fine textural details involving grain boundary relationship, grain morphology etc., whereas the EDS attachment of the scanning electron microscope was used for semi-quantitative analysis of different mineral phases. The instrument was operated with 20 kV acceleration voltage.

Quantitative mineral chemical data were acquired using a JEOL JXA 8530F Electron MicroProbe at Yokohama National University, Japan. The instrument was operated at 15 kV acceleration voltage using 20 nA specimen current. 1 μm probe diameter for the spot size was used for point analyses. Moreover, a complementary set of analysis of the same samples were done using JEOL JXA 8200 Superprobe at the Natural Science Center for Basic Research and Development (N-BARD), Hiroshima University, Japan. The operating conditions for the latter were 15 kV accelerating voltage, 20 nA beam current and 1-2μm beam diameter. Natural standards were used in both instruments and raw data were corrected by the ZAF program. Another set of samples were analyzed in a 4 spectrum Cameca SX-100 Electron Microprobe at the Electron Microprobe Facility of Department of Geology and Geophysics, IIT Kharagpur, India. The instrument was operated at 15 kV acceleration voltages using 15 nA specimen current. A 1-mm probe diameter for the spot size was used for point analyses.

5.2 Petrography

5.2.1 High-grade rocks of the Central Gneissic Belt

5.2.1.1 Felsic gneiss

Felsic gneiss is the most abundant rock type of the Central Gneissic Belt. In the outcrop-scale, the rock is light coloured with some amount of mafic minerals, which defines the foliation. The mineral constituents are quartz, alkali feldspar and plagioclase with varying amount of biotite, garnet, ilmenite and magnetite. Modal abundance of mafic mineral is usually low (<10 modal %). The rock shows pervasive foliation by flattening of grains (Fig.

5.1) which locally produces a mylonitic fabric. In mylonitized felsic gneiss, all the phases show extreme grain refinement. Alkali feldspar is perthitic in nature and constitutes the dominant feldspar species. Garnet grains show variation in size. Medium- to coarse garnet grains are highly fractured while those within the mylonitized rocks are tiny and irregular to extremely flat in shape and appears as sigma shaped clasts (Fig. 5.2). Fine biotite flakes and hornblende grains occur parallel to the foliation. A few small orthopyroxene grains are present within the foliation-parallel mafic bands. Zircon is abundant accessory phase within the matrix and the grains are elongated showing idioblastic shape.

5.2.1.2 Migmatitic hornblende gneiss

This rock type is the second most abundant rock type within the high-grade Central Gneissic Belt. This rock contains mafic minerals as observed in outcrop-scale. This rock is essentially composed of hornblende, alkali feldspar, plagioclase, quartz and accessory minerals like zircon and apatite (Fig. 5.3). In some samples, garnet and biotite are also observed. Foliation within the rock is mainly defined by alternate felsic and the mafic mineral layers. The rock is almost devoid of pyroxene. Plagioclase, alkali feldspar and ilmenite are present as inclusion within porphyroblastic hornblende (Fig. 5.4). In some samples (e.g. sample RNG102C), garnet porphyroblasts show intergrowth texture with Fe-Ti oxide minerals (Fig. 5.5). Features like subgrain boundaries and grain boundary migration are observed within large quartz grains. Alkali feldspar predominates over plagioclase feldspar. Alkali feldspar shows perthitic texture with plagioclase occurring as blebs and fine lamellae. Some antiperthitic plagioclase grains are also present. Myrmeckitic texture is present in some samples (Fig. 5.6). Biotite grains are present along the margin of large hornblende grains. Zircon is the principal accessory mineral. Size of this mineral ranges between 100-200 μm, and some unusually large sized (~300-400 μm long) zircon grains are also present.

5.2.1.3 Charnockite gneiss

Charnockite gneiss mainly occurs in the central part of the Central Gneissic Belt along an E-W trending ridge. The gneissic foliation in the rock is marked by alternate orthopyroxene + hornblende-rich dark and quartzofeldspathic light bands in outcrop-scale. This foliation changes to a mylonitic one in the vicinity of the major shear zones. The rock is medium-grained and greyish in colour. Dark bands contain orthopyroxene + hornblende + magnetite + ilmenite ± clinopyroxene ± biotite as well as accessory minerals like apatite and zircon in varying proportions. Minerals present in this rock are granoblastic (Fig. 5.7) and textures of magmatic crystallization, if any, have been completely obliterated due to granulite facies metamorphism. In few samples, coronal garnet (with intergrown quartz) is present, forming on orthopyroxene and ilmenite grains (Fig. 5.8). Minerals are mostly equigranular and medium-sized, although few porphyroblasts of perthitic feldspar are present (Fig. 5.9). Quartz grains within the leucoband are flat, showing subgrain formation and recrystallization by grain boundary migration. In most of the samples, orthopyroxene grains are replaced by hornblende along fractures and cleavage planes of the former (Fig. 5.10). Some hornblende grains occur along the mutual boundaries of orthopyroxene clusters (Fig. 5.11). Magnetite and ilmenite also occur along the boundaries of orthopyroxene. Dominant feldspar species within the charnockite gneiss is alkali feldspar (perthitic), though plagioclase is also present in varying amount in different samples.

5.2.1.4 Mafic granulite

Mafic granulite occurs as enclaves and lenses sporadically within the charnockite gneiss. The rock contains clinopyroxene, plagioclase, garnet, quartz, magnetite, ilmenite, orthopyroxene with variable amount of hornblende and biotite. The rock can be subdivided into two

mineralogical varieties, namely (i) garnet-bearing mafic granulite and (ii) garnet-free mafic granulite. The former variety of rock shows coarse granoblastic fabric consisting of garnet, clinopyroxene, ilmenite, plagioclase and quartz which locally shows transformation to a gneissic fabric. The mafic layer consists of garnet + clinopyroxene that show stretching and flattening along the foliation due to granulite facies metamorphism and deformation. Plagioclase forms the leucocratic layers. In sample RNG 122, garnet and clinopyroxene grains are extremely deformed (Fig. 5.12). The garnet + clinopyroxene + plagioclase + quartz + ilmenite assemblage represents the peak granulite stage. Tiny quartz and magnetite grains are present either as inclusion within garnet or as small matrix phases (Fig. 5.13). Clinopyroxene grains in sample RNG 132B show exsolved magnetite blebs (Fig. 5.14). Both clinopyroxene and garnet grains are variably replaced by hornblende and biotite. Garnet-free mafic granulite is mainly composed of orthopyroxene + clinopyroxene + plagioclase + ilmenite with subordinate amount of hornblende and biotite.

5.2.1.5 Amphibolite

Amphibolite occurs as enclaves within the migmatitic hornblende gneiss and the felsic gneiss. Most of the samples show a coarse granoblastic aggregate of hornblende and plagioclase with variable amount of garnet and quartz (Fig. 5.15). Both hornblende and plagioclase show recrystallization and polygonal structure. Biotite forms over hornblende and garnet defining a crude schistosity. Quartz forms small anhedral grains in the interstitial spaces of hornblende. Magnetite grains are often associated with garnet. In some other variety, garnet is absent, but clinopyroxene is present as relict (Fig. 5.16).

5.2.1.6 Metagabbro

Metagabbro is present as xenoliths within migmatitic hornblende gneiss and felsic gneiss. It is composed of plagioclase, clinopyroxene, orthopyroxene, hornblende and biotite with subordinate amount of magnetite. Plagioclase and pyroxene grains show interlocking arrangement and original igneous textures are preserved (Fig. 5.17). Plagioclase laths show inverse zoning. Exsolved lamellae and blebs of orthopyroxene are present within clinopyroxene (Fig. 5.18). Tiny recrystallized pyroxene grains occur along the margin of large plagioclase (Fig. 5.19). Small blebs of K-feldspar are present within plagioclase, showing anti-perthite texture. Intergrowth of hornblende is observed with orthopyroxene and magnetite is present as inclusion within orthopyroxene.

5.2.1.7 Calc-silicate granofels

Calc-silicate granofels occurs as dismembered boudins within the charnockite gneiss and is characterized by the assemblage plagioclase-garnet-quartz-epidote-sphene and accessory zircon. Garnet and epidote are medium-grained and occur as clusters (Fig. 5.20). Garnet shows characteristic orange colour. Quartz and few plagioclase grains occur as inclusion within the large garnet grains. Backscattered electron images of epidote show compositional zoning. Garnet porphyroblasts are surrounded by epidote grains. Euhedral zircon and subhedral sphene are present as inclusion within epidote.

5.2.1.8 Later intrusives

Mafic intrusives occur at several places within the Central Gneissic Belt. These are metadolerite in mineral composition containing clinopyroxene, orthopyroxene, plagioclase, Fe-Ti oxides, pyrite, amphibole and biotite. Relic igneous features like intergranular and ophitic textures are present (Fig. 5.21). Plagioclase is lath-shaped showing compositional

zoning. Although both pyroxenes are present, clinopyroxene is more abundant. The latter shows dusty exsolved blebs of Fe-Ti oxide. Clusters of amphibole and biotite replace clinopyroxene in a sequential pattern. All the phases show minor evidence of deformation, e.g. plagioclase laths show bending, marginal recrystallization and undulose extinction. However, intensity of metamorphism is low. Orthopyroxene is present as inclusion within large laths of plagioclase showing relic ophitic to subophitic textures (Fig. 5.22). Overall, the rock appears to be affected by low- grade metamorphism.

5.2.2 Low-grade supracrustal rocks

As discussed in chapter 3, the low-grade supracrustal rocks are essentially composed of quartzite, biotite-muscovite schist, calc-silicate schist and occasional presence of sillimanite-fibrolite-bearing schistose rock near the shear zone.

5.2.2.1 Quartzite

Quartzite of the Southern and the Northern Supracrustal Belts are composed of quartz and feldspar grains, with minor amount of biotite and muscovite. In some cases the distribution of minerals is unimodal. In other cases, the distribution is bimodal. In many samples, a crude foliation is defined by micaceous minerals (Fig. 5.23). Samples essentially composed of quartz with some amount of feldspar showing a textural maturity may have quartz arenite as its protolith. Evidence of deformation is evident from presence of mylonitic texture, quartz ribbon and polycrystalline quartz. Recrystallized quartz grains also show prominent S-C fabric near the shear zones. Development of fibrolite grain (Fig. 5.24) within quartzite is also observed in samples near shear zones.

5.2.2.2 Mica Schist

This rock shows green-schist facies mineral assemblage of muscovite + biotite + quartz + feldspar and occasional presence of Fe-Ti oxide minerals. In some samples, bimodal distribution of Fe-Ti oxide is observed, where one generation developed parallel to the schistose layering and another generation of massive Fe-Ti oxide grains are present. Muscovite and biotite grains are oriented along the foliation (Fig. 5.25). The rock is highly foliated and schistose in nature. Occasional presence of tourmaline is also observed. At the margin of the Southern Supracrustal Belt and the Central Gneissic Belt near the South Riamol Splay, the grade of metamorphism is found to increase to amphibolite grade. This is evident from the development of prismatic grains of andalusite, sillimanite-fibrolite needles, volumetric increase of magnetite and ilmenite within the rock. This may be attributed to the increase in temperature along shear zones that resulted in the breakdown of muscovite grains to skeletal alkali feldspar and fibrous aluminosilicates (Fig. 5.26). Muscovite from the pre-existing low-grade assemblage is also observed. In microscopic scale, the S-C fabric is defined by recrystallized quartz grains and some micro-scale intrafolial folds.

5.2.2.3 Calc-silicate schist

This rock shows green-schist facies assemblage of calcite + tremolite + actinolite + quartz ± scapolite ± diopside (Fig. 5.27). Occasionally, biotite and muscovite are also present. This rock is highly foliated and some samples the foliation is defined by tremolite crystals (Fig. 5.28). Deformational features like crenulation are present in some samples. The overall association in field suggests a sandstone-shale-limestone protolith for the rocks of the Southern Supracrustal Belt.

5.3 Mineral Chemistry

Mineral chemical data for the high-grade rocks of the Central Gneissic Belt were acquired (Table 5.2-5.10). No phase analysis for the low-grade supracrustal rocks was done.

5.3.1 Charnockite gneiss

Compositionally pyroxene grains in the charnockite gneiss are relatively Fe-rich. Some amount of clinopyroxene (augite) is also present along with orthopyroxene. Al content is negligible in both varieties but is higher in clinopyroxene. X_{Mg} [=Mg/(Mg+Fe^{2+})] in pyroxene varies between 0.23-0.37. Ferric iron is negligible with X_{Fe3+} [=Fe^{3+}/(Fe^{2+}+Fe^{3+})] varying between 0.011-0.055. Hornblende is compositionally hastingsite to ferrotschermakite (Leake et al., 1997) with X_{Mg} varying between 0.26 and 0.31. TiO_2 content varies within the range of 1.8 and 2.5 wt.%. F and Cl contents in hornblende are negligible. Feldspar grains are both albite and orthoclase in nature. Oxide minerals like ilmenite and magnetite are present within the charncokite gneiss samples, though ilmenite is the abundant species. X_{Fe3+} varies between 0.037 and 0.077. Ilmenite and orthopyroxene grains are closely associated and in many cases and show an interlocking texture.

5.3.2 Migmatitic hornblende gneiss

Hornblende grains in this rock are calcic and compositionally hastingsite (Leake et al., 1997). X_{Mg} of hornblende varies between 0.30-0.34. X_{Mg} of biotite varies between 0.29-0.33. TiO_2 content varies between 4-5 wt.%. F and Cl contents are negligible in both hornblende and biotite grains. Both phases are Mg-poor (X_{Mg} = 0.31-0.34), but Mg content increases towards the rim. Garnet grains in this sample are enriched in almandine-grossular (Alm$_{68-70}$Gr$_{18-20}$Sps$_{6-7}$Pyr$_{5-7}$) with negligible amount of uvarovite and andradite (<1 mole %).

5.3.3 Mafic granulite

Clinopyroxene is Mg-rich (X_{Mg} = 0.60-0.64) with rimward decrease of Mg content. X_{Fe3+} in the clinopyroxene varies between 0-0.16. Al_2O_3 content in the rim varies in the range 1.0-1.4 wt.%, whereas the cores contain up to 4.0 wt.%. Garnet is mainly almandine-grossular-pyrope ($Alm_{60-63}Grs_{19-22}Pyp_{14-16}Sps_{3-4}$) in nature, with almandine content increasing and pyrope content decreases towards the rim in garnet porphyroblasts. Feldspar is albitic in nature ($Ab_{61-69}An_{30-37}Or_{1.3-1.5}$). Hornblende is compositionally ferropargasite (Leake et al., 1997) with X_{Mg} varying in the range 0.45-0.48. Ti content increases in adjacent to plagioclase feldspar. Intergrowth of ilmenite observed within hornblende porphyroblast. Biotite (X_{Mg} = 0.42-0.50) contains high Ti (TiO_2 - 4.5-5.0 wt.%).

5.3.4 Calc-silicate granofels

Essentially composed of epidote, where Al-rich sample (22-24 wt.% Al_2O_3) and its Fe_2O_3 content varies in the range 0.72-0.82 wt.%, gradually increasing from core to rim. Garnet is Ca-rich and contains high amount of ferric iron [X_{Fe3+}= 0.82-0.86)] and shows compositional variation in terms of grossular-andradite ($Grs_{35-40}And_{51-57}$) components. Almandine component is low (6-8 mole%) but pyrope and spessartine components are negligible (<1 mole%). TiO_2 in garnet varies in the range 0.13-0.39 wt.%. Ca and Fe^{3+} contents of garnet decrease adjacent to epidote grains. Matrix is consists of plagioclase which shows compositional variation in the range $Ab_{54-60}An_{39-45}$.

5.3.5 Amphibolite

Hornblende grains are compositionally calcic-amphibole and are edenite to tschermakite in nature (Leake et al., 1997) and magnesian (X_{Mg} = 0.56 - 0.67). Small amount of TiO_2 (0.9-1.48 wt. %) is present and it is observed that Ti content in hornblende included within garnet

is higher than those in the matrix. Garnet composition varies among almandine (57-62 mole%), grossular (20-27 mole %) and pyrope (13-15 mole%) components. Spessartine component is much lower in comparison (<4 mole %). Grossular content increases from core towards the rim. Plagioclase composition is anorthite-rich (X_{An} = 0.58-0.60) with insignificant orthoclase (~1 mole %) component. Clinopyroxene is present in small quantity and is diopsidic in nature (X_{Mg} = 0.70-0.73). Na_2O (0.40 wt. %) and Al_2O_3 (1.14-1.16 wt.%) contents are low in clinopyroxene. Ilmenite is present as inclusion within garnet grains. This ilmenite is ferrian (Fe^{3+}/Fe^{2+} = 0.019) and contains small amount of Mg ($X_{Mg=}$ 0.02) as geikielite component.

5.3.6 Metagabbro

Hornblende grains are ferropargasite in composition (Leake et al., 1997). It shows an intergrowth relationship with orthopyroxene. Magnetite is present as inclusion within orthopyroxene. Clinopyroxene is magnesian (X_{Mg} = 0.66-0.69) and slightly aluminous (Al_2O_3 =3.0-3.5 wt.%) compared to orthopyroxene (Al_2O_3= 1.0-2.2 wt.%; X_{Mg}= 0.52-0.53) which occurs as intergrowth or as exsolved phase. Na_2O content is low in clinopyroxene (<1 wt.%). Exsolved orthopyroxene contains high amount of TiO_2= 2.2 wt.% and Al_2O_3 (1.7-2.0 wt. %) in comparison to the matrix grains.

5.3.7 Later intrusives

Clinopyroxene grains are magnesian (X_{Mg} = 0.64-0.70) compared to orthopyroxene (X_{Mg} = 0.45-0.48). Al_2O_3 content of matrix orthopyroxene is low (0.82-0.90 wt.%), whereas orthopyroxene inclusion within plagioclase contains high amount of Al_2O_3 (5.16 wt.%). Ca and Na contents of included orthopyroxene (1.34 wt.% and 0.65 wt.% respectively) are slightly higher than those present within the matrix. Clinopyroxene is low-Na variety

(Na_2O=0.53-1.1 wt.%). Al_2O_3 content in clinopyroxene (2.0-7.7 wt.%) is much higher compared to orthopyroxene and shows rim-ward decreasing trend when occurs adjacent to plagioclase grains. Biotite (X_{Mg}= 0.46-0.47) contains high amount of Ti (6.3-6.9 wt.% TiO_2). Fe-Ti oxide is magnetite, though small amount of Fe^{3+} (X_{Fe3+} =0.13-0.34) and Mn (0.34-0.67 wt.%) are also present. Minor amount of hornblende is present. Composition of hornblende varies from ferropargasite to magnesiohastingsite (Leake et al., 1997), with X_{Mg} of 0.50.

For the low-grade supracrustal rocks, mineral chemical analysis has not been acquired. The latter rocks are finer grained with mineral assemblages showing very high degree of freedom. Therefore, the peak metamorphic conditions are difficult to determine from these rocks.

5.4 Geothermobarometry

Pressure and temperature conditions of metamorphism for the studied rocks of the Central Gneissic Belt were determined from conventional geothermobarometric calculations as well as phase equilibria modelling. Peak P-T conditions for the mafic granulite were calculated using garnet-clinopyroxene- plagioclase-quartz assemblages in different samples. The garnet-clinopyroxene (Ganguly, 1979) thermometry yields peak temperature within the range 796-846°C at an assumed pressure of 10 kbar (Table 5.11) for different samples. The garnet-clinopyroxene-plagioclase-quartz barometer (Moecher et al., 1988) yields pressure estimates in a range between 9.0- 9.5 kbar (Di-barometer) and 12.8-13.2 kbar (Hd-barometer) for different samples. The silica-CaTs-An barometer (McCarthy and Patino Douce, 1998) yields pressures about 10.6 kbar. Mafic granulites underwent retrograde metamorphism and the P-T condition for this stage was estimated from the hornblende- and biotite-bearing assemblages. The hornblende-plagioclase thermometer (Holland and Blundy, 1994) yields temperature of 617-623°C at 8 kbar pressure whereas the Al-in-Hornblende barometer (Anderson and Smith,

1995) yields pressure in the range of 7.4-7.5 kbar with an input temperature range of 600-620°C. The garnet-biotite thermometer (Dasgupta et al., 1991) yields 700-736°C at 6.5 kbar pressure for different samples.

Peak metamorphic temperature of the charnockite gneiss was deduced from the orthopyroxene-ilmenite assemblage after the model of Bishop et al. (1980) which yields temperatures in the range 746-842°C at 8 kbar. Peak pressure condition was recorded from the clinopyroxene-plagioclase assemblages using the model of silica-CaTs-anorthite barometer (McCarthy and Patino Douce, 1998) which yields pressure about 7.2 kbar at an assumed temperature of 840°C (Table 5.11).

For the hornblende migmatitic gneiss, the plagioclase-hornblende assemblage yields peak temperature of 695°C at 8 kbar pressure (Holland & Blundy, 1994). The garnet-ilmenite thermometer (Pownceby et al., 1987) yields 673°C at 6.5 kbar whereas the garnet-biotite thermometer (Dasgupta et al., 1991) estimated a maximum temperature of 695°C at the same assumed pressure. The Al-in-hornblende barometry (Anderson and Smith, 1995) yields a maximum pressure of 6.20 kbar at an assumed temperature of 695°C (Table 5.11).

Relict mineral assemblage of garnet-clinopyroxene within amphibolite yields a maximum temperature of 718°C at an assumed pressure of 8 kbar using the model of Ganguly (1979). The hornblende-plagioclase thermometer (Holland and Blundy, 1994), on the other hand, yields 578-610°C temperatures. Metagabbro, which occurs as enclaves within the granite gneiss, yields a peak metamorphism temperature of 763°C estimated from the hornblende-plagioclase thermometer (Holland and Blundy, 1994). Coexisting pyroxene pairs from the same sample records a temperature within the range of 653-664°C (Kretz, 1982), which can be considered as a reset value. Al-in hornblende barometry (Anderson and Smith, 1995) yields pressure of 6.9 kbar at an assumed temperature of 760°C (Table 5.11).

From the estimated P-T data (Table 5.11), it is clear that the mafic granulites from Central Gneissic Belt underwent a high-pressure metamorphism (up to 10.6 kbar) followed by a phase of cooling. The drop in metamorphic temperature (ΔT) at this stage was > 200°C (850-623°C) with a drop in pressure (ΔP) of ~3.5 kbar (Table 5.11). From the thermo-barometric data, it can also be inferred that metagabbro, amphibolite and charnockite gneiss underwent metamorphism at lower pressure and temperature conditions. However, it was observed that the temperature estimates in almost all the calculations yield low values presumably due to resetting during subsequent cooling. To retrieve the actual P-T conditions, the technique of phase diagram modelling was adopted.

5.5 Phase diagram modelling

Apart from the conventional geothermobarometric approach, evolutionary history of some of the key rocks of the Central Gneissic Belt was unravelled by phase diagram modelling using the program Perple_X version 6.6.8 (Connolly and Petrini, 2002). These phase diagrams were calculated as functions of pressure and temperature using the technique of free energy minimization (Connolly, 2005). One sample each from the mafic granulite and the amphibolite were used for this purpose. Phase diagram modelling for the charnockite gneiss is not shown here as the mineral assemblage of this rock shows high variance over extended P-T regions. Sample RNG-122 represents the mafic granulite where the peak metamorphic assemblage is characterized by the assemblage Grt+Cpx+Pl+Qtz+Opx. The other sample RNG 144 represents the amphibolite with the peak assemblage of Hbl+Pl+Qtz+Grt+Cpx. XRF data were chosen as the initial bulk compositions for these two samples (Table 6.1). Phase diagram calculations were done with the Na_2O-CaO-FeO-MgO-Al_2O_3-SiO_2-TiO_2-H_2O system using hp02ver.dat data file. Fe_2O_3 was not chosen as a component since presence of Fe^{3+} in ferromagnesian phases is minor. Solid solution models (file solute_07.dat) for garnet,

orthopyroxene and clinopyroxene were taken from Holland and Powell (1998), while the model of Newton et al. (1980) was taken for plagioclase. For clinoamphibole, the model of Dale et al. (2005) was used. There is no appropriate melt model for metabasic systems. It was considered that the assemblages on the high-temperature side of the phase diagrams may be metastable with respect to assemblages involving melt, or at least coexist with the melt. However, experimental work, calculations and natural observations suggest that the topology of the phase relationships is similar when mineral assemblages coexist with fluid (H_2O) or melt and that the field boundaries may not move significantly (e.g. Wolf and Wyllie, 1994; Vielzeuf and Schmidt, 2001; Pattison et al., 2003).

P-T phase diagrams (Fig. 5.29a, b) were calculated and contoured with modal percentages of key solid solution phases in order to bracket the conditions of peak metamorphic conditions within the broad stability fields of high variance assemblages. For the sample RNG 122, the modal percentages of garnet and plagioclase were calculated with the Perplex software. Percentage of garnet and plagioclase were also computed using modal analysis and the values are 14-18% and 33-37% respectively. These modal values were compared with theoretically calculated isopleths in figure 5.29c and a P-T window of 10.6±0.5 kbar, 860±20ºC is defined to represent the peak metamorphic condition. For the sample RNG 144, modal percentages of garnet and plagioclase were measured as 1-3% and 25-28% respectively. When these values were compared with the theoretically calculated isopleths in figure 5.29d, the peak P-T window of 8.5±0.2 kbar, 800±20ºC is indicated.
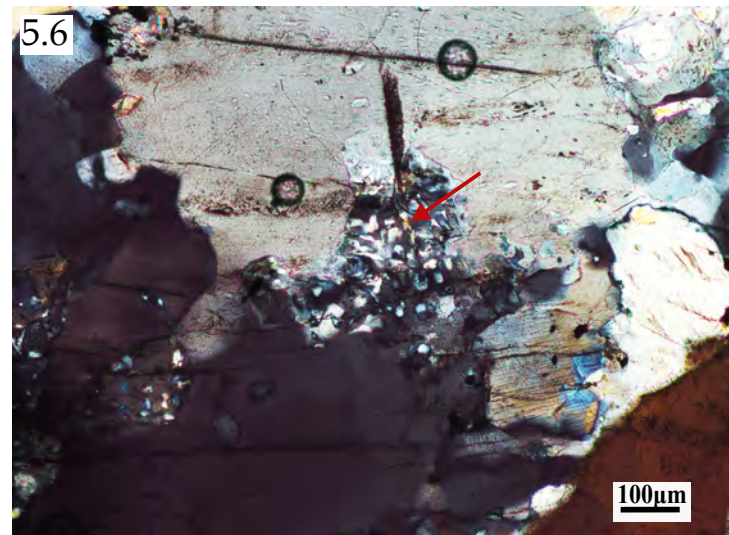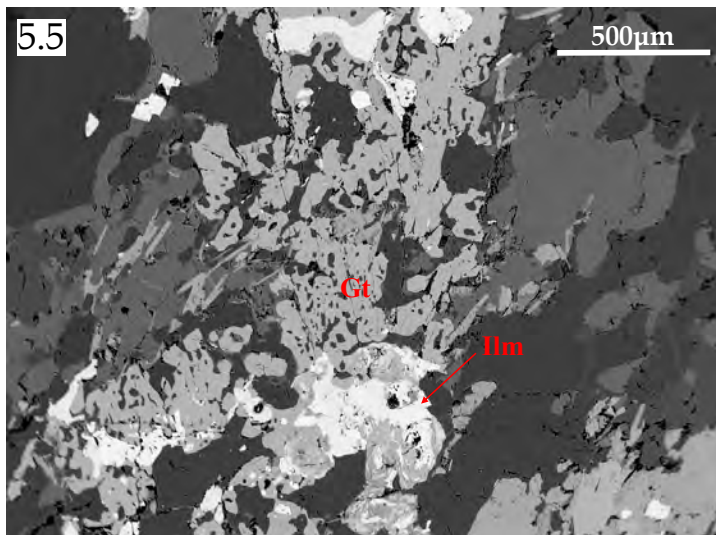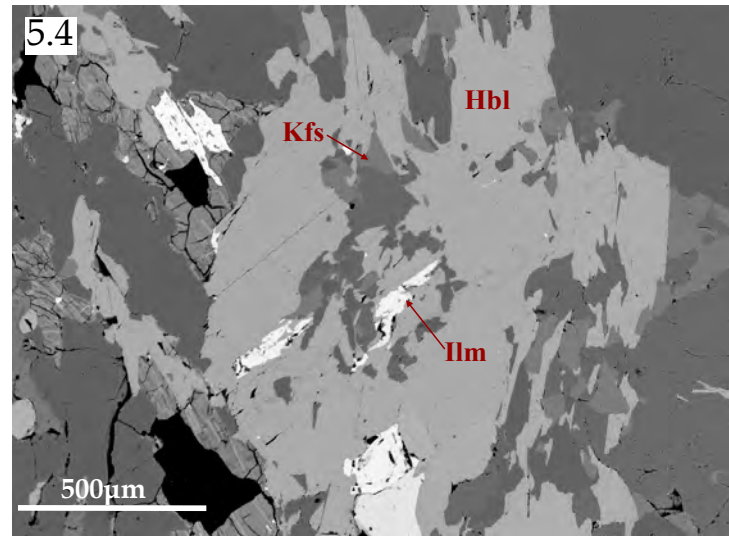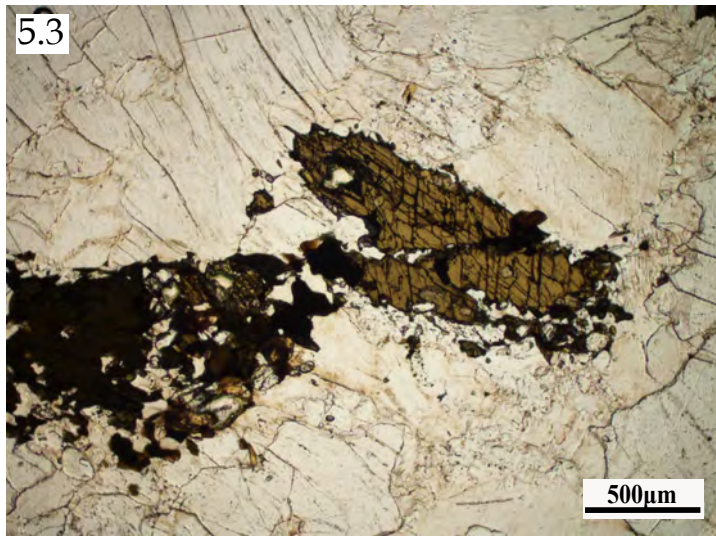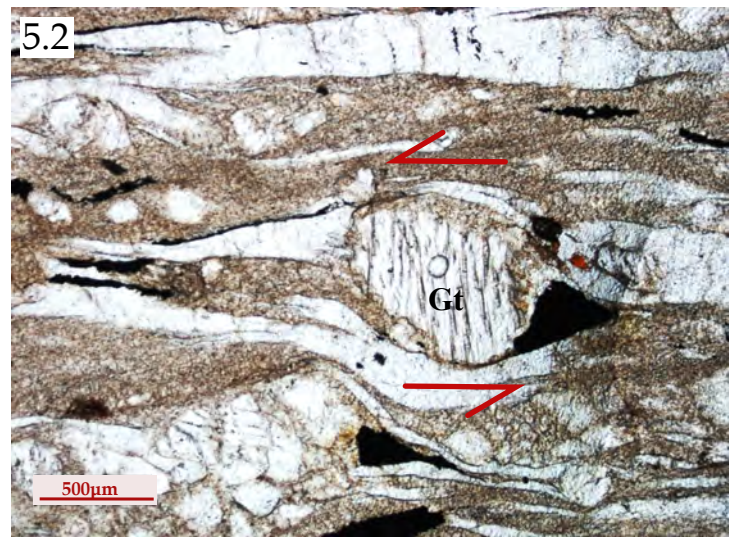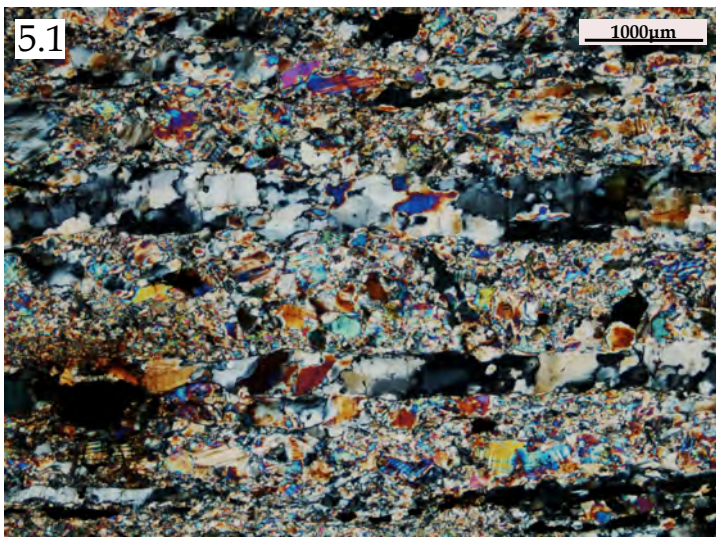
Photomicrograph and BSE image depicting Fig. (5.1) Mylonitic texture developed in felsic gneiss sample. (5.2) Rotation of garnet porphyroblast present in mylonitised felsic gneiss. (5.3) Migmatitic hornblende gneiss. (5.4) Alkali feldspar and ilmenite present as inclusion within porphyroblastic hornblende (5.5) occasional presence of garnet and intergrowth between garnet and ilmenite. (5.6) Myrmekitic texture (arrow) within alkali feldspar in migmatitic hornblende gneiss.
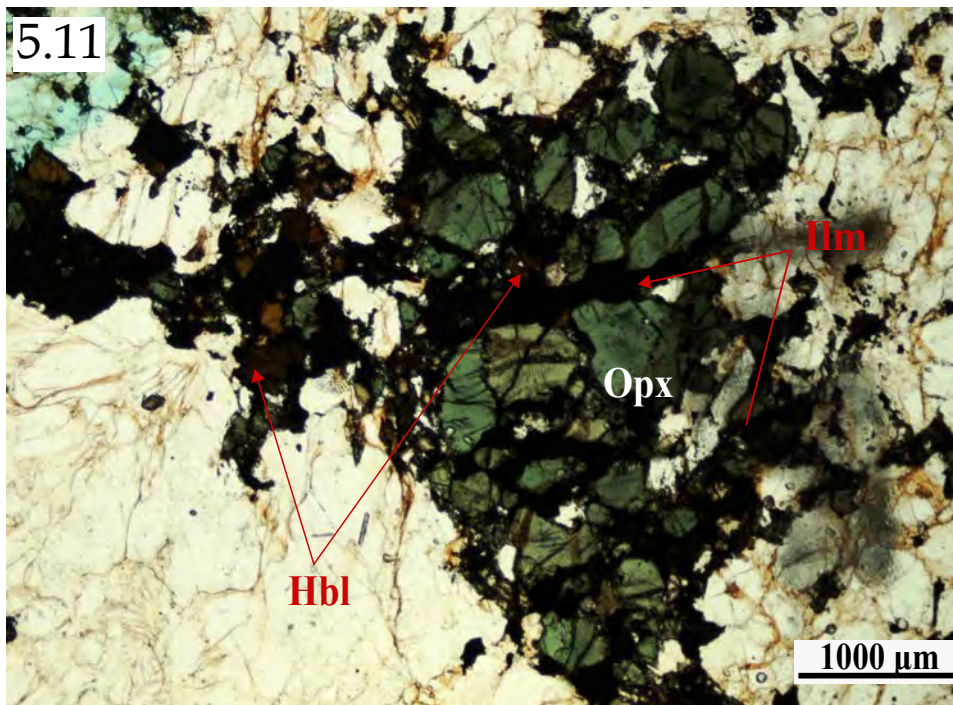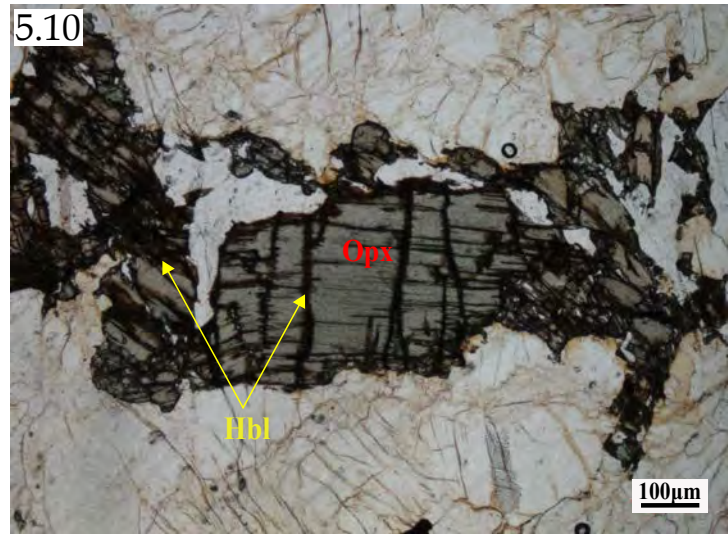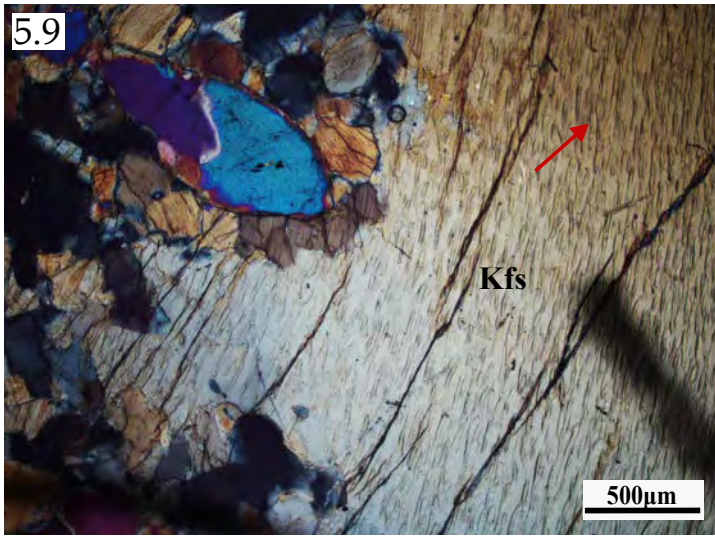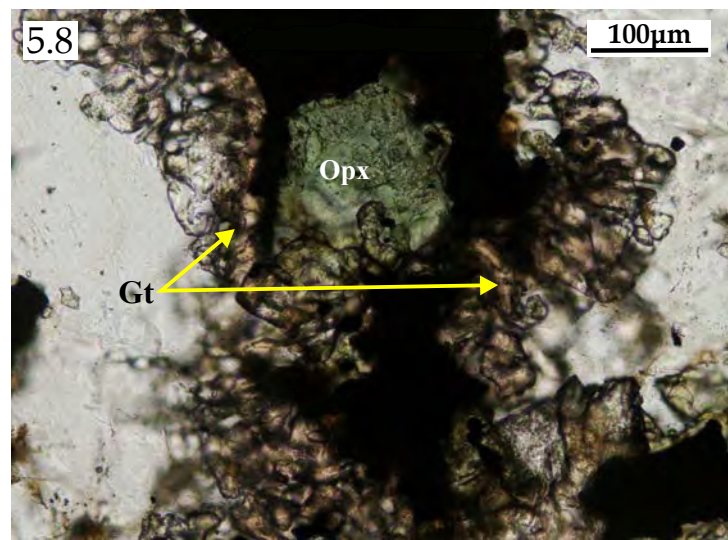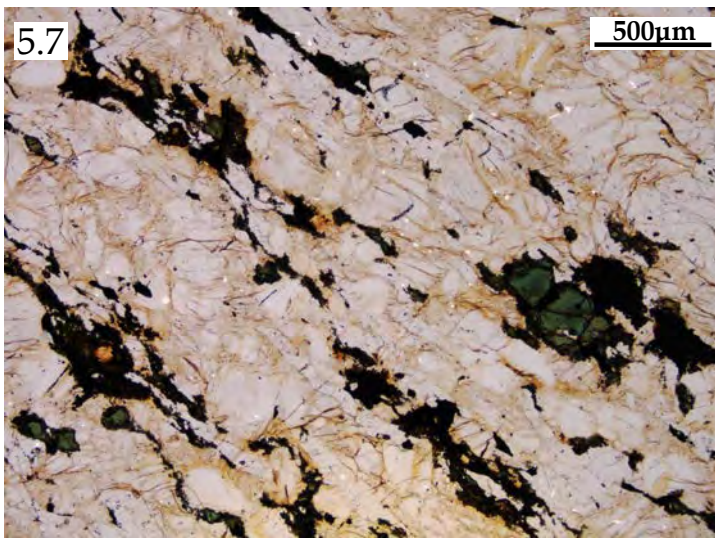
Photomicrograph depicting Fig. (5.7) Overall granoblastic texture in charnockite. (5.8) Presence of garnet in charnockite. Garnet occur as coronal structure around orthopyroxene grains.
(5.9) Perthitic texture (arrow) observed in alkali feldspar porphyroblast in charnockite samples.
(5.10) Replacement of orthopyroxene grains by hornblende along clevage and fracture planes.
(5.11) Hornblende and ilmenite grains occur along the mutual boundaries of orthopyroxene clusters.
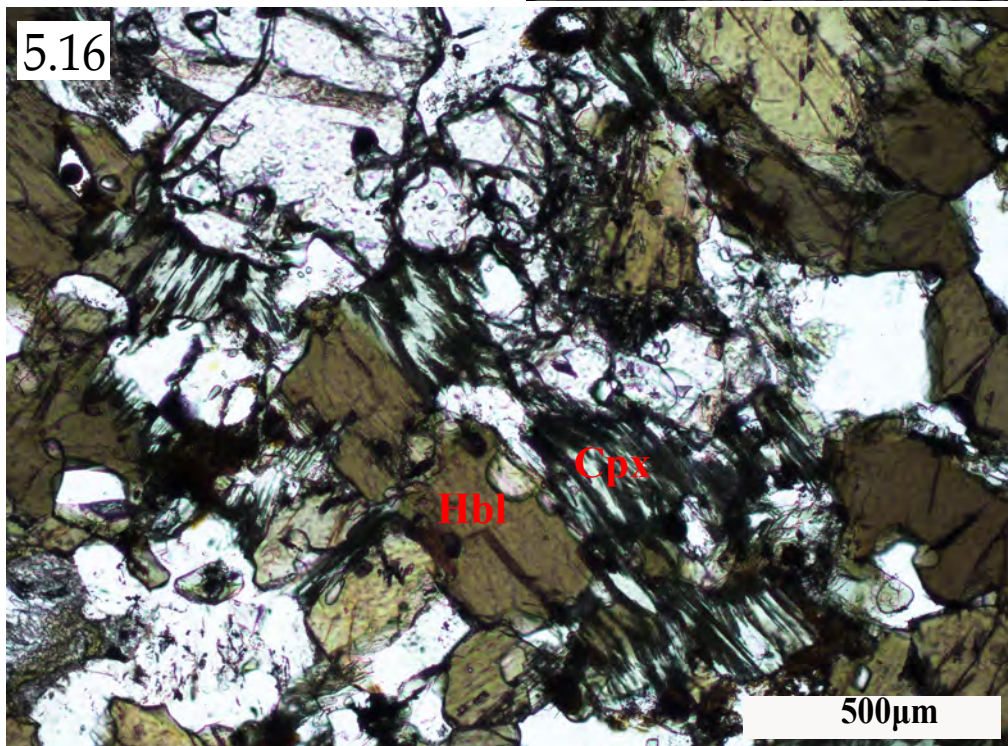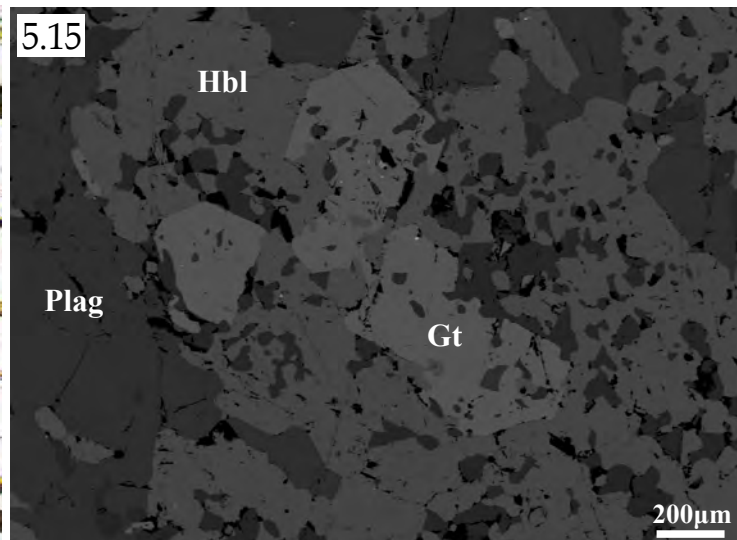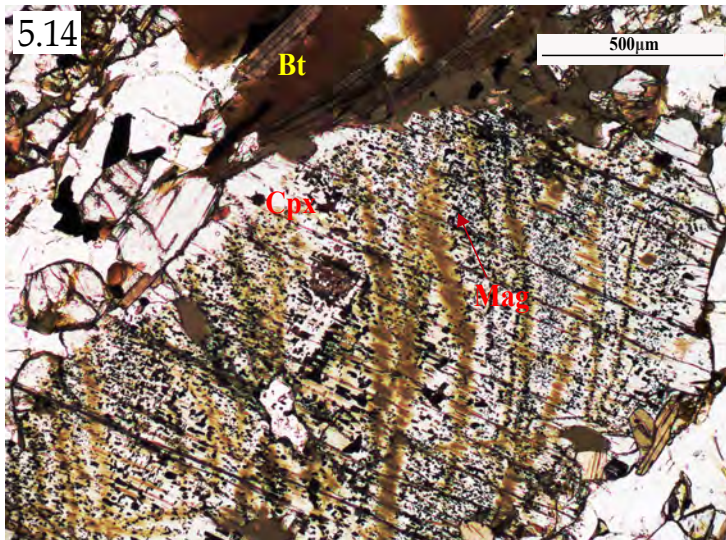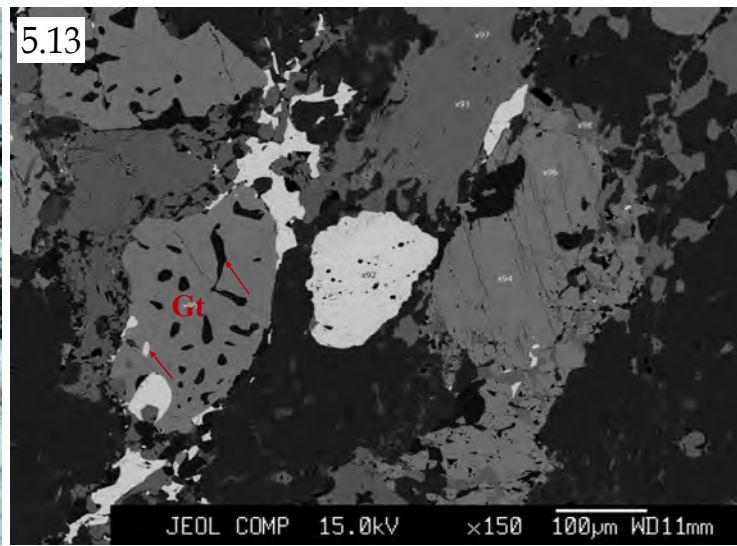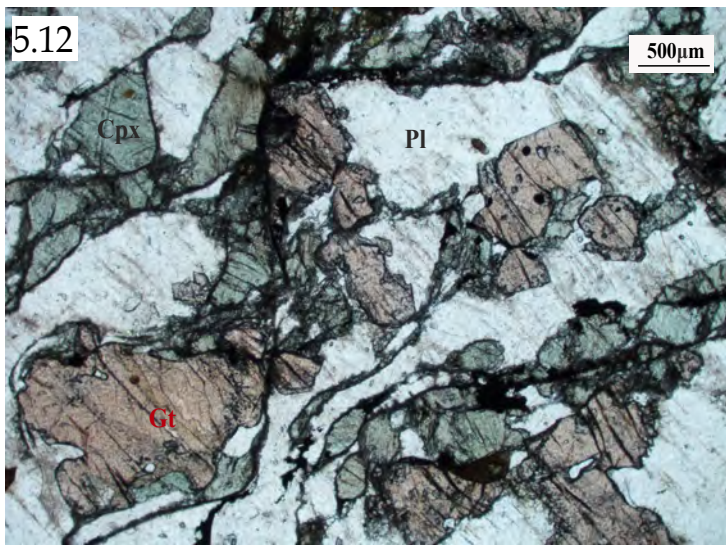
Photomicrograph and BSE image depicting Fig. (5.12) Deformed clinopyroxene and garnet grains in mafic granulite. (5.13) Intergrowth of quartz and magnetite grains within garnet. (5.14) Magnetite blebs within clinopyroxene porphyroblast. (5.15) Hornblende, plagioclase and garnet showing granoblastic texture in amphibolite. (5.16) Relict clinopyroxene in amphibolite sample.
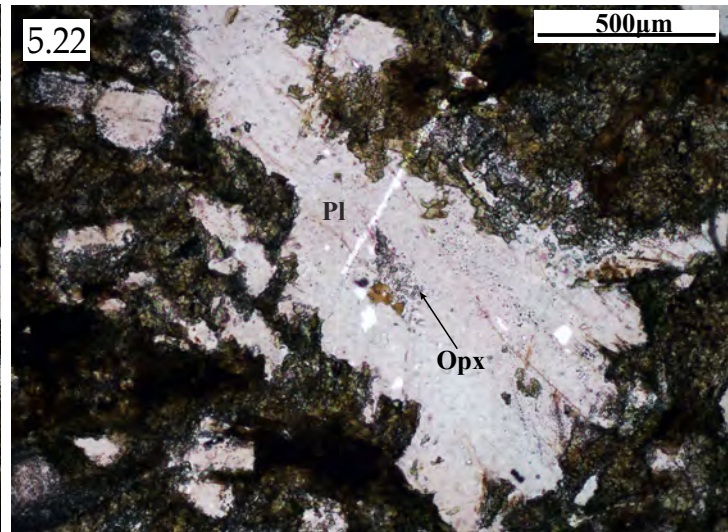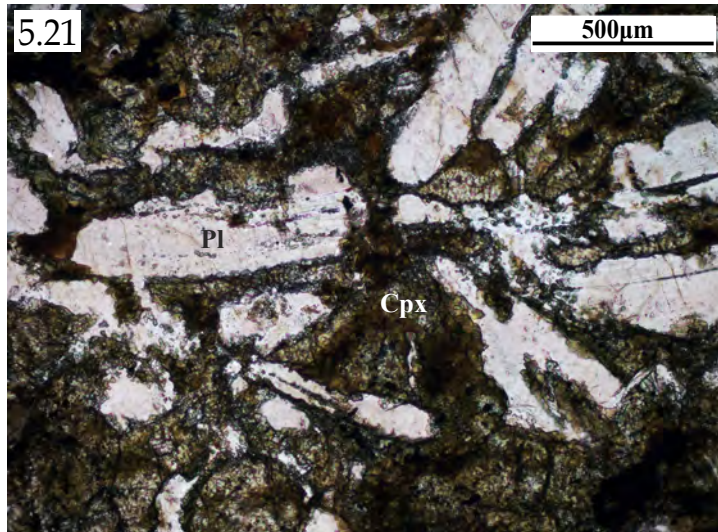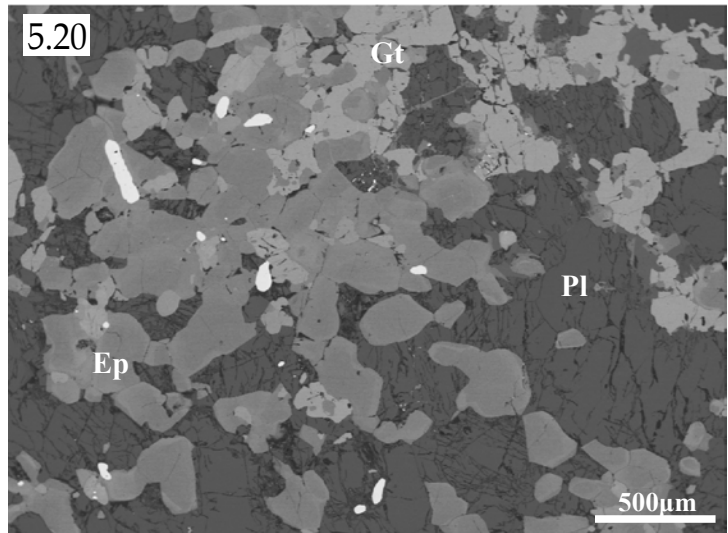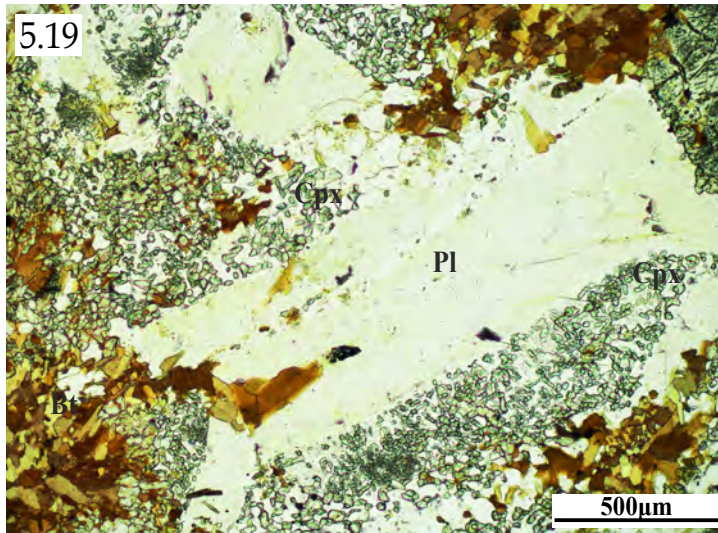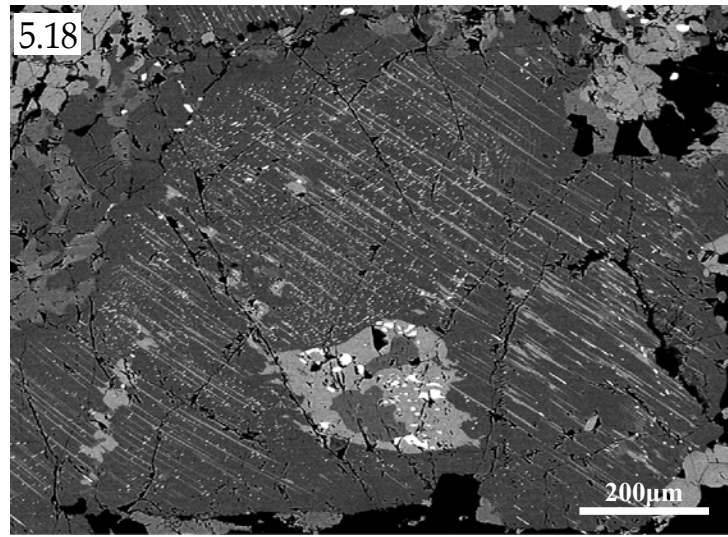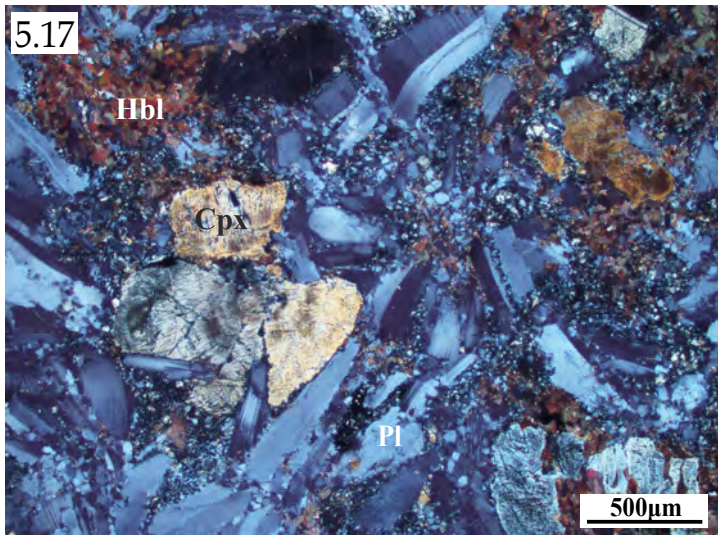
Photomicrograph and BSE image depicting Fig. (5.17) Relict igneous interlocking texture in metagabbro. (5.18) Exsolved lamellae of orthopyroxene within clinopyroxene in metagabbro sample. (5.19) Tiny recrystallized pyroxene grains occur along the margin of large plagioclase in metagabbro. (5.20) Calc-silicate granofels sample showing granoblastic texture and aggragate of garnet, plagioclase and epidote. (5.21) Relict igneous textures (ophitic and sub-ophitic) preserved within metadolerite. (5.22) Orthopyroxene inclusion within large laths of plagioclase.
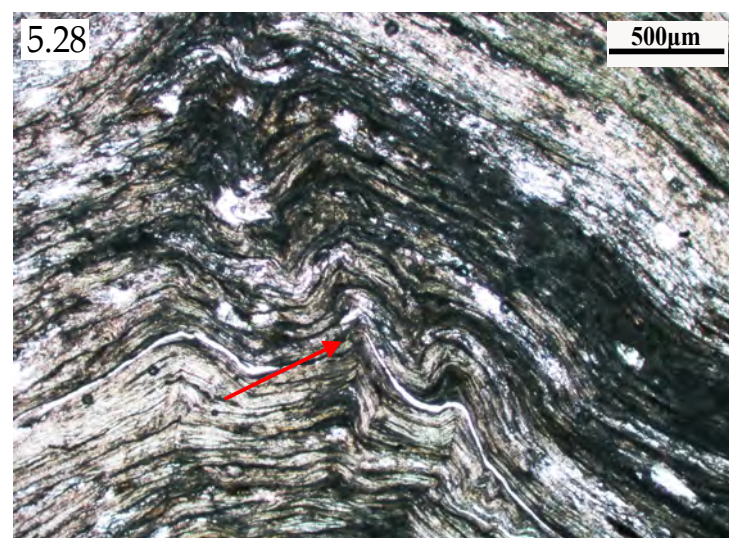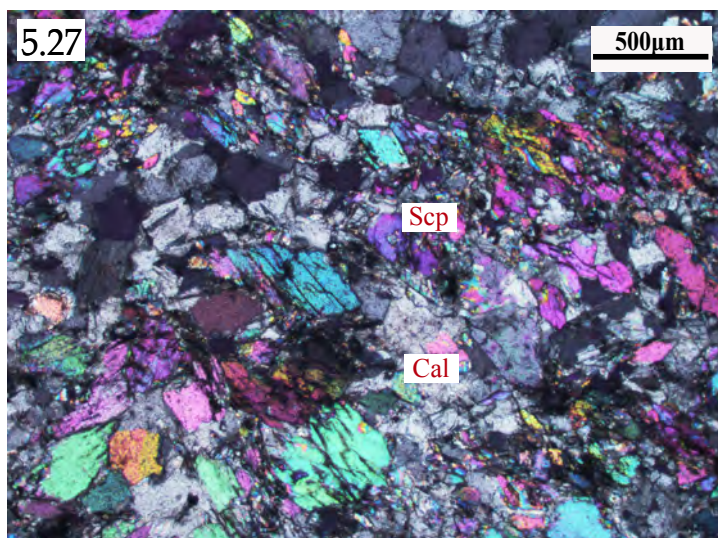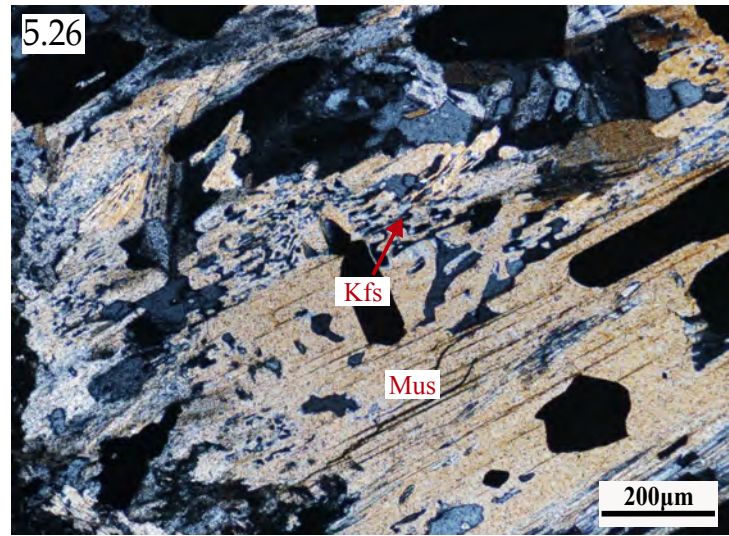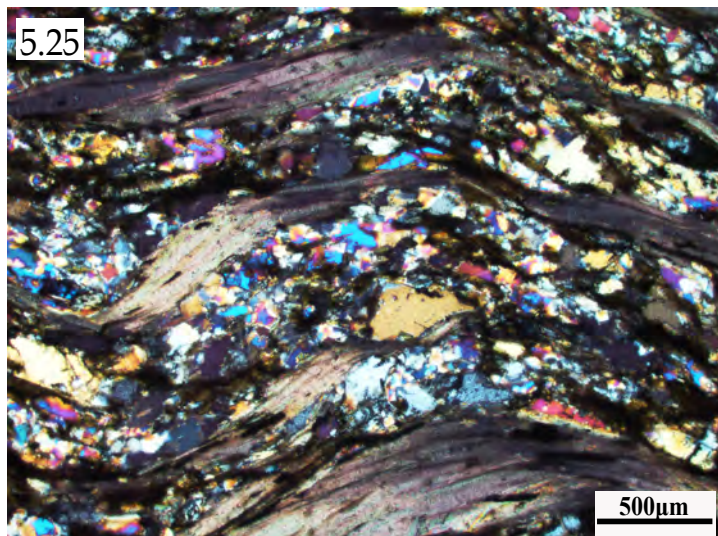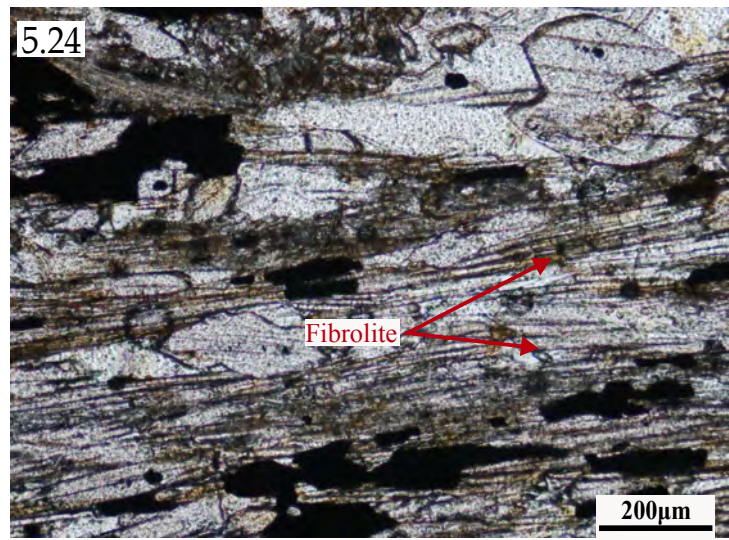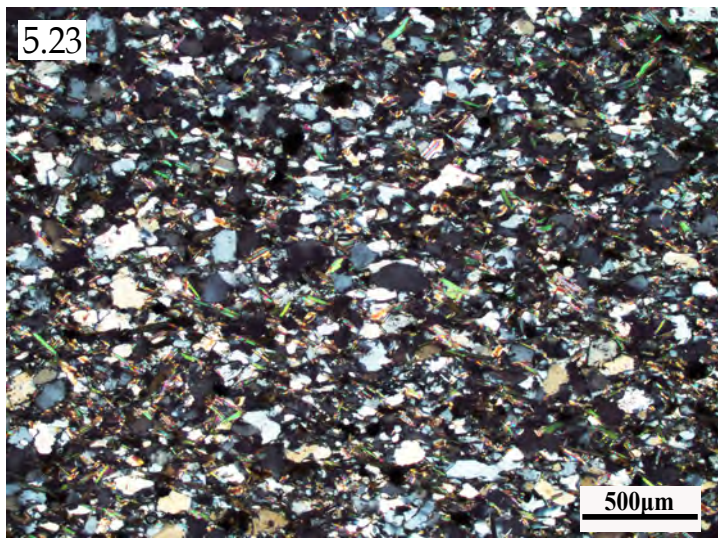
Photomicrograph depicting Fig. (5.23) Quartzite with muscovite defining crude foliation. (5.24) development of fibrolite within quartzite. (5.25) Muscovite defining foliation within mica-schist. (5.26) Breakdown of mucovite and development of skeletal alkali feldspar and fibrolite in mica-schist. (5.27) Calc-silicate schist. (5.28) Development of crenulation (arrow) in calc-silicate schist.
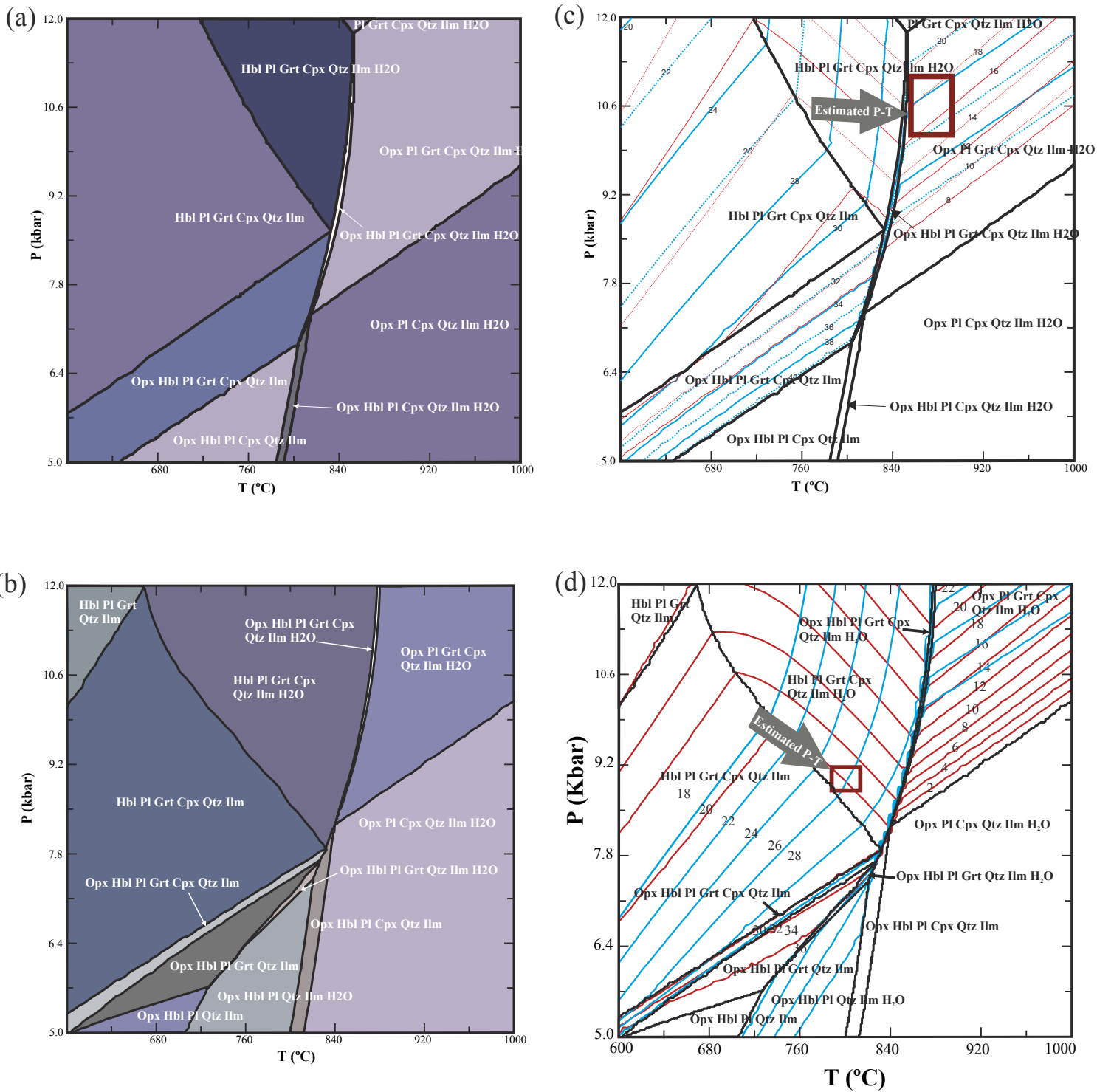
Fig. 5.29: P-T pseudo-sections constructed at calculated bulk compositions from representative studied samples to demonstrate P-T evolution of mafic granulite (a) and amphibolite (b). Compositional isopleths were constructed using calculated modal percentage values from the two samples (c,d). Bulk compositions for each were taken from whole rock XRF data presented in Table 6.1.

Table 5.1: Mineralogy of the studied rock types from the Central Gnessic Belt and the supracrustal belts

Sample No.	Rock type	Qtz	K-Feld	Plag	Hbl	Bt	Mus	Opx	Cpx	Gt	Mag	Ilm	Zr	Spn	Cal	Ep	Scp	Trem	Sil-Fib	Texture
RNG 50D	Leucogranite	✓	✓	✓			✓			✓			✓							Post kinematic Gt; weak foliation
RNG 51	Felsic Gneiss	✓	✓			✓			✓	✓	✓		✓							Gt porphyroblast; evidence of deformation
RNG 175		✓	✓		✓	✓							✓							
RNG 54D		✓	✓	✓						✓		✓	✓							Mylonitic foliation
RNG102C	Migmatitic Hbl Gneiss	✓	✓	✓	✓	✓				✓	✓	✓								Gt-Ilmintergrowth
RNG123A		✓	✓	✓	✓	✓							✓							Foliated
RNG129B		✓	✓	✓		✓						✓	✓							deformed Hbl grains
RNG146C		✓	✓	✓	✓	✓							✓							Perthitic & myrmekitic texture; Bt present along margin of Hbl
RNG158	Charnockite	✓	✓		✓			✓	✓		✓	✓								Highly foliated, quartz grains streched in nature, development of foliation parallel Fe-Ti oxide
RNG120A		✓	✓		✓	✓		✓	✓		✓	✓	✓							Granoblastc texture
RNG129A		✓	✓		✓	✓		✓				✓	✓							
RNG165		✓	✓		✓			✓	✓	✓		✓								Coronal Gt growth around Opx grains
RNG53E		✓	✓		✓			✓				✓								Development of Hbl at the margin of Opx
RNG133		✓	✓		✓	✓		✓			✓	✓								
RNG144A	Amphibolite	✓		✓	✓							✓				✓				
RNG 278B		✓	✓	✓	✓				✓		✓	✓								Intergrowth texture within Kfs; breakdown of Px grain along margin.
RNG 283		✓		✓	✓	✓			✓	✓	✓									Granoblastic texture; Symplectite like texture between Hbl-qtz.
RNG 122	Mafic Granulite	✓	✓	✓	✓			✓	✓	✓	✓	✓	✓							overall granoblastic fabric; inclusion of qtz within gt grains.
RNG 132B		✓		✓	✓	✓	✓	✓	✓	✓		✓								Exsolved magnetite blebs within Cpx grains.
RNG 157B		✓		✓	✓	✓		✓	✓			✓								
RNG 145B	Meta dolerite	✓		✓	✓			✓	✓			✓								No preferred orientation; ophitic to sub-ophitic texture.
RNG 52B		✓		✓	✓	✓			✓											In some cases poikilitic texture observed.
RNG 53D		✓		✓	✓			✓	✓			✓								
RNG 214	Metagabbro	✓		✓	✓	✓		✓	✓		✓									Relict igneous texture preserved;
RNG 144C		✓		✓	✓			✓	✓		✓	✓								
RNG 278A	Calc-silicate granofels	✓		✓					✓				✓	✓		✓				Occur as boudins within charnockite; Ep & Gt occur as cluster.
RNG 266A		✓													✓			✓		Granofelsic texture;
RNG 143	Pegmatite	✓	✓	✓		✓	✓						✓							
RNG 27	Quartzite	✓	✓				✓												✓	
RNG 136		✓				✓														Crude foliation defined by mica
RNG 143B		✓	✓	✓			✓						✓							
RNG 150A		✓																		Mylonitic texture
RNG 268		✓											✓							
RNG 270A		✓	✓	✓			✓						✓							Develkopment of fibrolitegrains
RNG 151C	Calc-silicste, tremolite schist	✓							✓						✓	✓				
RNG 151D		✓				✓	✓								✓			✓		Development of crenulation clevage
RNG 151E		✓													✓			✓		
RNG 142F	Mus-Bt Schist	✓	✓			✓	✓													Highly schistose in nature
RNG 143C		✓	✓			✓	✓					✓								Bimodal distribution of Fe-Tl
RNG 151F		✓	✓			✓	✓					✓								Dvelopment of alumino-silicate minerals and breakdown of muscovite grains to skeletal K-feldspar
RNG 209	Fibrolite	✓	✓				✓				✓								✓	

Table 5.2 Representative chemical composition of pyroxene in charnockite (RNG 120A) sample

Analysis No.	4	5	6	13	17	20	25	31	32	38	40
SiO2	47.889	47.367	50.469	48.25	47.706	48.106	48.051	50.3	48.848	48.378	54.768
TiO2	0.041	0.032	0.096	0	0.092	0.134	0.052	0.087	0.009	0.073	0.031
Al2O3	0.289	0.287	0.743	0.299	0.291	0.26	0.292	0.791	0.25	0.282	0.253
FeO	41.912	41.312	21.216	42.054	42.662	42.876	42.183	21.199	42.871	42.844	32.691
MnO	1.033	0.794	0.339	0.866	0.997	0.881	0.973	0.502	1.112	1.021	0.581
MgO	7.369	7.232	6.619	7.506	7.221	7.8	7.845	6.529	7.753	7.983	6.699
CaO	0.932	0.833	19.716	0.83	0.803	0.656	0.815	20.114	0.785	0.648	5.961
Na2O	0.025	0.014	0.477	0.001	0.02	0.038	0.038	0.471	0.012	0.029	0.086
K2O	0	0.003	0	0.015	0	0.003	0.014	0.032	0	0	0.008
P2O5	0	0.002	0	0.019	0	0	0.029	0	0.055	0.019	0
Cl	0	0.031	0	0	0	0	0	0	0.059	0.073	0.024
F	0	0.006	0	0	0	0.005	0.014	0	0.017	0.002	0.005
Total	99.49	97.913	99.674	99.84	99.791	100.759	100.305	100.025	101.77	101.352	101.109

O basis   **6**

	4	5	6	13	17	20	25	31	32	38	40
Si	1.991	2.002	1.992	1.998	1.981	1.973	1.978	1.979	1.986	1.972	2.202
Ti	0.001	0.001	0.003	0.000	0.003	0.004	0.002	0.003	0.000	0.002	0.001
Al	0.014	0.014	0.035	0.015	0.014	0.013	0.014	0.037	0.012	0.014	0.012
Cr	0.000	0.000	0.000	0.000	0.000	0.000	0.000	0.000	0.000	0.000	0.000
Fe3+	0.004	0.000	0.013	0.000	0.019	0.036	0.031	0.039	0.016	0.040	0.000
Fe2+	1.454	1.460	0.687	1.456	1.463	1.435	1.420	0.659	1.442	1.421	1.099
Mn	0.036	0.028	0.011	0.030	0.035	0.031	0.034	0.017	0.038	0.035	0.020
Mg	0.457	0.456	0.389	0.463	0.447	0.477	0.481	0.383	0.470	0.485	0.402
Ca	0.042	0.038	0.834	0.037	0.036	0.029	0.036	0.848	0.034	0.028	0.257
Na	0.002	0.001	0.036	0.000	0.002	0.003	0.003	0.036	0.001	0.002	0.007
K	0.000	0.000	0.000	0.001	0.000	0.000	0.001	0.002	0.000	0.000	0.000
Total	4.000	4.000	4.000	4.000	4.000	4.000	4.000	4.000	4.000	4.000	4.000
XMg	0.239	0.238	0.362	0.241	0.234	0.250	0.253	0.368	0.246	0.254	0.268
XFe^{3+}	0.002	0.000	0.019	0.000	0.013	0.025	0.022	0.055	0.011	0.027	0.000

$X_{Mg}=Mg/[Mg+Fe^{2+}]$; $X_{Fe3+} = Fe^{3+}/[Fe^{2+}+Fe^{3+}]$;

Table 5.2 Representative chemical composition of hornblende in charnockite (RNG 120A) sample

Analysis No.	1	15	21	23	26	27	36	41
SiO2	40.538	39.156	40.531	40.11	40.267	40.751	39.986	40.682
TiO2	1.794	2.516	2	2.411	1.632	1.631	2.19	2.163
Al2O3	10.104	10.303	10.347	10.467	10.248	10.607	10.489	10.449
FeO	26.22	25.865	25.38	26.404	26.908	26.378	26.51	26.16
MnO	0.158	0.121	0.132	0.295	0.323	0.268	0.195	0.183
MgO	4.807	4.217	4.871	4.479	4.733	4.878	4.623	4.796
CaO	10.49	10.474	10.409	10.672	10.53	10.584	10.68	10.592
Na2O	1.693	1.589	1.727	1.815	1.676	1.426	1.758	1.807
K2O	1.384	1.472	1.379	1.519	1.309	1.361	1.613	1.573
P2O5	0	0.048	0	0	0	0	0.002	0
Cl	0.132	0.208	0.111	0.096	0.107	0.021	0.095	0.068
F	0	0.002	0	0	0.011	0.009	0	0.005
Total	97.32	95.971	96.887	98.268	97.743	97.914	98.141	98.476

O basis				23				
Si	6.348	6.268	6.361	6.262	6.276	6.304	6.246	6.311
Al iv	1.652	1.732	1.639	1.738	1.724	1.696	1.754	1.689
Al vi	0.212	0.212	0.275	0.188	0.159	0.238	0.177	0.221
Ti	0.211	0.303	0.236	0.283	0.191	0.190	0.257	0.252
Cr	0.000	0.000	0.000	0.000	0.000	0.000	0.000	0.000
Fe3+	0.707	0.528	0.589	0.561	0.898	0.874	0.633	0.588
Fe2+	2.726	2.935	2.743	2.886	2.609	2.538	2.830	2.805
Mn	0.021	0.016	0.018	0.039	0.043	0.035	0.026	0.024
Mg	1.122	1.006	1.140	1.042	1.100	1.125	1.077	1.109
Ca	1.760	1.796	1.750	1.785	1.758	1.754	1.787	1.760
Na	0.514	0.493	0.526	0.549	0.507	0.428	0.532	0.543
K	0.276	0.301	0.276	0.303	0.260	0.269	0.321	0.311
F	0.000	0.001	0.000	0.000	0.005	0.004	0.000	0.002
Cl	0.035	0.056	0.030	0.025	0.028	0.006	0.025	0.018
OH*	1.965	1.943	1.970	1.975	1.966	1.990	1.975	1.980
Total	17.550	17.590	17.552	17.637	17.525	17.450	17.641	17.615
X_{Mg}	0.292	0.255	0.294	0.265	0.297	0.307	0.276	0.283
X_{Fe3+}	0.206	0.152	0.177	0.163	0.256	0.256	0.183	0.173

$X_{Mg} = Mg/[Mg+Fe^{2+})]$; $X_{Fe3+} = Fe^{3+}/[Fe^{2+}+Fe^{3+})]$;

Table 5.2 Representative chemical composition of feldspar in charnockite (RNG 120A) sample

Analysis No.	8	9	11	12	19	22	24	28	30	33	34	35	43
SiO2	64.343	63.695	64.043	64.562	65.037	65.499	65.211	65.114	64.724	64.85	64.702	64.41	65.061
TiO2	0.022	0	0	0	0.062	0	0.009	0	0	0	0	0.046	0
Al2O3	18.315	23.031	23.059	18.329	18.608	18.643	18.53	18.507	18.451	18.542	22.581	23.471	18.524
FeO	0.121	0.084	0	0.017	0.524	0.036	0.316	0.254	0.406	0.056	0.145	0	0.228
MnO	0	0	0.002	0	0.024	0	0.083	0.021	0	0.092	0.042	0.02	0
MgO	0.009	0.01	0.013	0.011	0.053	0.03	0.022	0.005	0.019	0.007	0.02	0.01	0.017
CaO	0.042	4.163	3.894	0	0.014	0.075	0.007	0.032	0.013	0.013	3.837	4.205	0.005
Na2O	1.186	9.287	9.336	1.339	1.482	2.362	1.139	1.748	1.377	1.104	9.457	9.28	1.013
K2O	14.609	0.168	0.096	14.556	14.006	12.695	14.795	13.889	14.3	14.905	0.073	0.253	14.774
P2O5	0.044	0.011	0	0.011	0.038	0	0	0.001	0	0.055	0	0	0.003
Cl	0.01	0	0	0	0.03	0.006	0.001	0	0.018	0.021	0.002	0.031	0.056
F	0.009	0.017	0.014	0	0.011	0	0.011	0.015	0	0.002	0	0	0
Total	98.709	100.466	100.457	98.825	99.89	99.346	100.125	99.587	99.307	99.647	100.858	101.726	99.682
O basis							**8**						
Si	2.996	2.803	2.813	3.000	2.989	3.003	2.996	2.998	2.993	2.995	2.831	2.799	3.000
Al	1.005	1.195	1.194	1.004	1.008	1.007	1.004	1.004	1.006	1.009	1.165	1.202	1.007
Ti	0.001	0.000	0.000	0.000	0.002	0.000	0.000	0.000	0.000	0.000	0.000	0.002	0.000
Fe	0.005	0.003	0.000	0.001	0.020	0.001	0.012	0.010	0.016	0.002	0.005	0.000	0.009
Mn	0.000	0.000	0.000	0.000	0.001	0.000	0.003	0.001	0.000	0.004	0.002	0.001	0.000
Mg	0.001	0.001	0.001	0.001	0.004	0.002	0.002	0.000	0.001	0.000	0.001	0.001	0.001
Ca	0.002	0.196	0.183	0.000	0.001	0.004	0.000	0.002	0.001	0.001	0.180	0.196	0.000
Na	0.107	0.792	0.795	0.121	0.132	0.210	0.101	0.156	0.123	0.099	0.802	0.782	0.091
K	0.868	0.009	0.005	0.863	0.821	0.742	0.867	0.816	0.843	0.878	0.004	0.014	0.869
P	0.002	0.000	0.000	0.000	0.001	0.000	0.000	0.000	0.002	0.000	0.000	0.000	0.000
Total	4.986	5.000	4.991	4.989	4.979	4.970	4.986	4.986	4.985	4.989	4.990	4.996	4.976
Or	88.824	0.945	0.547	87.732	86.081	77.652	89.491	83.804	87.173	89.821	0.413	1.414	90.537
Ab	10.962	79.390	80.824	12.268	13.846	21.963	10.473	16.033	12.761	10.114	81.348	78.844	9.437
An	0.215	19.666	18.629	0.000	0.072	0.385	0.036	0.162	0.067	0.066	18.239	19.742	0.026
Xan	0.0021	0.1967	0.1863	0.0000	0.0007	0.0039	0.0004	0.0016	0.0007	0.0007	0.1824	0.1974	0.0003
Xab	0.1096	0.7939	0.8082	0.1227	0.1385	0.2196	0.1047	0.1603	0.1276	0.1011	0.8135	0.7884	0.0944
Xor	0.8882	0.0094	0.0055	0.8773	0.8608	0.7765	0.8949	0.8380	0.8717	0.8982	0.0041	0.0141	0.9054

XAn = Ca/(Ca+Na+K); XAb = Na/(Ca+Na+K); XOr = K/(Ca+Na+K)

Table 5.2 Representative chemical composition of ilmenite in charnockite (RNG 120A) sample

Analysis No.	2	18	39
SiO2	0	0.052	0.025
TiO2	49.788	51.19	50.828
Al2O3	0.148	0.216	0.138
FeO	47.53	46.882	47.121
MnO	0.549	0.7	0.596
MgO	0.168	0.118	0.188
CaO	0.031	0.012	0.032
Na2O	0.049	0	0
K2O	0.017	0.018	0
P2O5	0	0.017	0
Cl	0.002	0.007	0.024
F	0.014	0.02	0.018
Total	98.297	99.231	98.97

O basis		3	
Si	0.000	0.005	0.003
Ti	3.834	3.909	3.889
Al	0.018	0.026	0.017
Cr	0.000	0.000	0.000
Fe3+	0.313	0.146	0.201
Fe2+	3.758	3.834	3.808
Mn	0.048	0.060	0.051
Mg	0.026	0.018	0.029
Ca	0.003	0.001	0.003
Zn	0.000	0.000	0.000
Ba	0.000	0.000	0.000
Na	0.005	0.000	0.000
K	0.001	0.001	0.000
P	0.000	0.001	0.000
Total	8.000	8.000	8.000
XMg	0.007	0.005	0.007
XFe3+	0.077	0.037	0.050
Fe3+/Fe2+	0.083	0.038	0.053

$X_{Mg} = Mg/[Mg+Fe^{2+}]$; $X_{Fe3+} = Fe^{3+}/[Fe^{2+}+Fe^{3+}]$;

Table 5.3: Representative chemical composition of hornblende in migmatitic hornblende gneiss (RNG 146C) sample

Analysis No.	1	14	22	23	32
SiO2	40.25	40.426	40.809	40.557	40.476
TiO2	1.873	1.979	1.824	1.745	2.04
Al2O3	10.745	10.43	10.428	10.396	10.671
FeO	25.522	25.364	26.024	26.045	24.986
MnO	0.525	0.411	0.528	0.49	0.571
MgO	5.301	5.2	5.534	5.228	5.283
CaO	10.627	10.761	10.753	10.597	10.61
Na2O	1.759	1.701	1.757	1.832	1.807
K2O	1.361	1.399	1.353	1.524	1.444
P2O5	0.044	0.001	0	0.01	0
Cl	0.038	0.026	0.051	0.065	0.049
F	0.007	0	0.002	0	0
Total	**98.053**	**97.7**	**99.064**	**98.491**	**97.937**
O basis			23		
Si	6.228	6.292	6.246	6.268	6.276
Al iv	1.772	1.708	1.754	1.732	1.724
Al vi	0.188	0.206	0.128	0.162	0.226
Ti	0.218	0.232	0.210	0.203	0.238
Fe3+	0.828	0.658	0.894	0.805	0.668
Fe2+	2.475	2.644	2.438	2.562	2.572
Mn	0.069	0.054	0.068	0.064	0.075
Mg	1.223	1.207	1.263	1.205	1.221
Ca	1.762	1.795	1.763	1.755	1.763
Na	0.528	0.513	0.521	0.549	0.543
K	0.269	0.278	0.264	0.300	0.286
F	0.019	0.013	0.000	0.005	0.000
Cl	0.010	0.007	0.013	0.017	0.013
OH*	1.971	1.980	1.987	1.978	1.987
Total	17.558	17.586	17.549	17.604	17.591
X_{Mg}	0.331	0.313	0.341	0.320	0.322
X_{Fe3+}	0.251	0.199	0.268	0.239	0.206
Total Al	1.960	1.913	1.881	1.894	1.950

$X_{Mg} = Mg/[Mg+Fe^{2+})]$; $X_{Fe3+} = Fe^{3+}/[Fe^{2+}+Fe^{3+})]$;

Table 5.3: Representative chemical composition of biotite in migmatitic hornblende gneiss (RNG 146C) sample

Analysis No.	5	6	7	16	26	30	33
SiO2	34.91	35.078	34.849	35.638	35.211	35.372	35.481
TiO2	5.058	4.882	4.745	4.681	5.182	5.693	5.237
Al2O3	13.312	13.753	13.56	13.668	13.524	13.317	12.725
FeO	26.298	25.739	25.677	26.927	26.149	26.925	26.879
MnO	0.272	0.128	0.161	0.099	0.115	0.183	0.245
MgO	6.247	6.862	6.931	6.809	6.393	6.041	6.425
CaO	0.022	0	0	0.031	0.06	0.007	0.045
Na2O	0.145	0.071	0.1	0.115	0.135	0.135	0.085
K2O	8.977	9.195	8.991	9.044	8.919	9.277	8.946
P2O5	0.019	0	0	0.017	0.004	0	0
Cl	0.062	0.056	0.044	0.021	0.054	0.055	0.039
F	0	0	0.018	0	0	0	0
Total	95.324	95.763	95.075	97.05	95.744	97.005	96.108
O basis				**22**			
Si	5.550	5.528	5.532	5.555	5.553	5.535	5.598
Al iv	2.450	2.472	2.468	2.445	2.447	2.456	2.366
Al vi	0.044	0.082	0.070	0.066	0.067	0.000	0.000
Ti	0.605	0.579	0.567	0.549	0.615	0.670	0.621
Fe	3.496	3.392	3.409	3.510	3.449	3.524	3.547
Mn	0.037	0.017	0.022	0.013	0.015	0.024	0.033
Mg	1.480	1.612	1.640	1.582	1.503	1.409	1.511
Ca	0.004	0.000	0.000	0.005	0.010	0.001	0.008
Na	0.045	0.022	0.031	0.035	0.041	0.041	0.026
K	1.820	1.848	1.821	1.798	1.794	1.852	1.800
OH*	3.983	3.985	3.979	3.994	3.984	3.985	3.990
F	0.000	0.000	0.009	0.000	0.002	0.000	0.000
Cl	0.017	0.015	0.012	0.006	0.014	0.015	0.010
Total	19.531	19.552	19.558	19.557	19.493	19.513	19.510
Al total	2.494	2.554	2.537	2.511	2.514	2.456	2.366
XMg	0.297	0.322	0.325	0.311	0.304	0.286	0.299

$XMg = Mg/[Mg+Fe^{2+})]$; $XFe^{3+} = Fe^{3+}/[Fe^{2+}+Fe^{3+})]$;

Table 5.3: Representative chemical composition of feldspar in migmatitic hornblende gneiss (RNG 146C) sample

Analysis No.	10	11	12	17	20	24	31	34	25
SiO2	63.593	64.399	64.41	64.659	65.574	65.238	64.92	65.135	64.142
TiO2	0.017	0	0	0	0.002	0	0	0	0
Al2O3	17.798	18.259	18.296	18.309	18.654	18.532	18.305	18.507	23.126
FeO	1.936	0.174	0.246	0.565	0.15	0.243	0.821	0.348	0.1
MnO	0.123	0	0	0	0	0	0.102	0.013	0
MgO	0.162	0	0.016	0.124	0.016	0.007	0.1	0	0
CaO	0.196	0	0.024	0.088	0.001	0	0.005	0.011	4.125
Na2O	0.868	1.595	1.062	1.206	1.375	1.043	2.146	1.58	9.216
K2O	13.931	14.219	14.801	14.4	14.261	15.212	13.614	14.648	0.15
P2O5	0.016	0	0.016	0	0	0.014	0	0	0.015
Cl	0	0.012	0.001	0.007	0.001	0.008	0.044	0.022	0.006
F	0.017	0.011	0	0	0.02	0	0	0	0
Total	98.656	98.671	98.871	99.359	100.053	100.297	100.058	100.265	100.879
O basis					**8**				
Si	2.982	2.998	2.997	2.994	3.003	2.996	2.985	2.991	2.808
Al	0.984	1.002	1.003	0.999	1.007	1.003	0.992	1.002	1.193
Ti	0.001	0.000	0.000	0.000	0.000	0.000	0.000	0.000	0.000
Fe	0.076	0.007	0.010	0.022	0.006	0.009	0.032	0.013	0.004
Mn	0.005	0.000	0.000	0.000	0.000	0.000	0.004	0.001	0.000
Mg	0.011	0.000	0.001	0.009	0.001	0.000	0.007	0.000	0.000
Ca	0.010	0.000	0.001	0.004	0.000	0.000	0.000	0.001	0.193
Na	0.079	0.144	0.096	0.108	0.122	0.093	0.191	0.141	0.782
K	0.833	0.844	0.878	0.850	0.833	0.891	0.798	0.858	0.008
Total	4.981	4.995	4.987	4.986	4.971	4.994	5.011	5.006	4.990
Or	90.372	85.432	90.055	88.304	87.212	90.561	80.649	85.866	0.851
Ab	8.560	14.568	9.823	11.242	12.783	9.439	19.326	14.080	79.488
An	1.068	0.000	0.123	0.453	0.005	0.000	0.025	0.054	19.661
Xor	0.904	0.854	0.901	0.883	0.872	0.906	0.806	0.859	0.009
Xab	0.086	0.146	0.098	0.112	0.128	0.094	0.193	0.141	0.795
Xan	0.011	0.000	0.001	0.005	0.000	0.000	0.000	0.001	0.197

$XAn = Ca/(Ca+Na+K)$; $XAb = Na/(Ca+Na+K)$; $XOr = K/(Ca+Na+K)$

Table 5.4: Representative chemical composition of hornblende in migmatitic hornblende gneiss (RNG 102C) sample

Analysis No.	2	5	17	24	26	28
SiO2	40.279	40.821	40.63	40.36	40.535	40.986
TiO2	1.888	2.042	2.045	1.791	1.937	1.549
Al2O3	10.591	11.145	10.799	10.239	10.747	10.976
FeO	24.709	25.055	24.806	24.743	25.915	23.146
MnO	0.454	0.324	0.159	0.288	0.24	0.197
MgO	5.023	5.064	5.047	5.187	5.029	6.016
CaO	10.378	10.484	10.631	10.819	10.609	11.008
Na2O	1.798	1.81	1.659	1.714	1.835	1.787
K2O	1.443	1.47	1.416	1.49	1.487	1.348
P2O5	0.016	0	0.036	0.012	0.024	0
F	0	0.005	0.007	0	0	0.005
Cl	0.04	0.112	0.047	0.083	0.084	0.077
Total	96.618	98.333	97.283	96.726	98.441	97.096
O basis			23			
Si	6.330	6.297	6.341	6.364	6.271	6.375
Al iv	1.670	1.703	1.659	1.636	1.729	1.625
Al vi	0.292	0.324	0.327	0.267	0.230	0.387
Ti	0.223	0.237	0.240	0.212	0.225	0.181
Cr	0.000	0.000	0.000	0.000	0.000	0.000
Fe3+	0.599	0.609	0.513	0.465	0.687	0.400
Fe2+	2.648	2.624	2.725	2.798	2.666	2.611
Mn	0.060	0.042	0.021	0.038	0.031	0.026
Mg	1.177	1.165	1.174	1.219	1.160	1.395
Ca	1.747	1.733	1.778	1.828	1.758	1.834
Na	0.548	0.541	0.502	0.524	0.550	0.539
K	0.289	0.289	0.282	0.300	0.293	0.267
F	0.000	0.002	0.003	0.000	0.000	0.002
Cl	0.011	0.029	0.012	0.022	0.022	0.020
OH*	1.989	1.968	1.984	1.978	1.978	1.977
Total	17.585	17.564	17.562	17.652	17.602	17.641
X_{Mg}	0.308	0.307	0.301	0.304	0.303	0.348
X_{Fe3+}	0.185	0.188	0.158	0.142	0.205	0.133

$X_{Mg}=Mg/[Mg+Fe^{2+})]$; $X_{Fe3+} = Fe^{3+}/[Fe^{2+}+Fe^{3+})]$;

Table 5.4: Representative chemical composition of garnet in migmatitic hornblende gneiss (RNG 102C) sample

Analysis No.	12	15	20	21	23	30	36
SiO2	37.114	37.352	36.947	37.156	37.068	37.14	37.205
TiO2	0.05	0	0.043	0.001	0	0.045	0.053
Al2O3	20.059	20.344	19.964	20.264	20.042	19.935	20.004
FeO	30.704	30.37	32.097	30.883	30.489	31.388	31.48
MnO	3.06	2.928	2.903	2.843	2.88	2.676	2.48
MgO	1.305	1.66	1.419	1.402	1.41	1.373	1.373
CaO	6.94	6.662	6.82	6.752	6.757	6.812	6.636
Na2O	0.012	0.004	0.033	0.018	0.011	0.045	0
K2O	0.011	0	0.02	0.007	0.007	0	0
P2O5	0	0	0	0	0	0	0
F	0	0.002	0.009	0	0.009	0.002	0
Cl	0	0.003	0.046	0.092	0.034	0.004	0.031
Total	99.255	99.325	100.301	99.418	98.707	99.419	99.262

O basis				12			
Si	3.016	3.024	2.979	3.015	3.027	3.016	3.025
Ti	0.003	0.000	0.003	0.000	0.000	0.003	0.003
Al	1.921	1.941	1.897	1.938	1.929	1.908	1.917
Cr	0.000	0.000	0.000	0.000	0.000	0.000	0.000
Fe3+	0.041	0.011	0.141	0.033	0.017	0.056	0.028
Fe2+	2.046	2.045	2.023	2.063	2.065	2.075	2.113
Mn	0.211	0.201	0.198	0.195	0.199	0.184	0.171
Mg	0.158	0.200	0.171	0.170	0.172	0.166	0.166
Ca	0.604	0.578	0.589	0.587	0.591	0.593	0.578
Total	8.000	8.000	8.000	8.000	8.000	8.000	8.000
X^{Mg}	0.072	0.089	0.078	0.076	0.077	0.074	0.073
X^{Fe3+}	0.981	0.995	0.935	0.984	0.992	0.974	0.987
Almandine	67.772	67.625	67.870	68.424	68.217	68.763	69.774
Spessartine	6.976	6.640	6.649	6.481	6.581	6.097	5.640
Pyrope	5.237	6.625	5.720	5.625	5.671	5.506	5.496
Grossular	19.601	19.000	18.397	19.147	19.358	19.076	18.820
Andradite	0.414	0.110	1.364	0.323	0.173	0.558	0.271
Uvarovite	0.000	0.000	0.000	0.000	0	0.000	0.000

$X_{Mg} = Mg/[Mg+Fe^{2+})]$; $X_{Fe3+} = Fe^{3+}/[Fe^{2+}+Fe^{3+})]$;

$X_{Alm} = Fe2+/(Fe2+ + Mg+ Mn+ Ca)$; $X_{Prp} = Mg/(Fe2+ +Mg + Mn+Ca)$; $X_{Grs} = Ca/(Fe2+ +Mg +Mn +Ca)$.

$X_{Sps} = Mn/(Fe2+ +Mg +Mn +Ca)$.

Table 5.4: Representative chemical composition of biotite in migmatitic hornblende gneiss (RNG 102C) sample

Analysis No.	1	7	9	13	19	22	29
SiO_2	34.685	35.211	35.334	34.592	34.457	34.492	35.056
TiO_2	5.351	5.2	5.746	4.759	4.584	4.8	5.066
Al_2O_3	13.327	13.297	13.935	13.255	13.088	13.18	13.334
FeO	26.681	26.114	26.084	27.704	27.252	26.901	27.386
MnO	0.091	0.253	0.182	0.035	0.079	0.025	0
MgO	6.003	5.983	5.611	5.853	6.272	5.997	6.263
CaO	0.022	0.048	0.057	0.051	0.04	0.03	0.041
Na_2O	0.067	0.23	0.106	0.117	0.092	0.156	0.099
K_2O	9.1	8.996	8.997	8.731	8.771	8.865	9.044
P_2O_5	0	0	0	0.005	0	0	0.011
F	0.005	0	0	0	0	0	0.002
Cl	0.045	0.066	0.045	0.047	0.001	0.084	0.066
Total	95.378	95.398	96.097	95.149	94.636	94.53	96.368
O basis				22			
Si	5.521	5.583	5.545	5.537	5.538	5.547	5.530
Al iv	2.479	2.417	2.455	2.463	2.462	2.453	2.470
Al vi	0.021	0.069	0.123	0.038	0.017	0.045	0.010
Ti	0.641	0.620	0.678	0.573	0.554	0.581	0.601
Cr	0.000	0.000	0.000	0.000	0.000	0.000	0.000
Fe	3.552	3.463	3.424	3.709	3.663	3.618	3.613
Mn	0.012	0.034	0.024	0.005	0.011	0.003	0.000
Mg	1.424	1.414	1.313	1.397	1.503	1.438	1.473
Ca	0.004	0.008	0.010	0.009	0.007	0.005	0.007
Na	0.021	0.071	0.032	0.036	0.029	0.049	0.030
K	1.848	1.820	1.801	1.783	1.798	1.818	1.820
OH*	3.985	3.982	3.988	3.987	4.000	3.977	3.981
F	0.003	0.000	0.000	0.000	0.000	0.000	0.001
Cl	0.012	0.018	0.012	0.013	0.000	0.023	0.018
Total	19.522	19.499	19.404	19.549	19.582	19.557	19.554
Al total	2.500	2.485	2.578	2.501	2.479	2.498	2.479
X_{Mg}	1.825	1.823	1.696	1.773	1.913	1.835	1.880

$X_{Mg} = Mg/[Mg+Fe^{2+}]$; $X_{Fe3+} = Fe^{3+}/[Fe^{2+}+Fe^{3+}]$;

Table 5.4: Representative chemical composition of ilmenite in migmatitic hornblende gneiss (RNG 102C) sample

Analysis No.	4	8	16	34	35
SiO2	0	0.031	0.029	0.018	0.108
TiO2	49.087	10.717	51.365	49.504	25.649
Al2O3	0.156	0.411	0.17	0.182	4.444
FeO	45.487	79.578	44.189	46.062	62.384
MnO	0.997	0.483	0.65	0.707	0.653
MgO	0.118	0.022	0.143	0.044	0.137
CaO	0.046	0.085	0.023	0	0.022
Na2O	0.017	0.007	0.018	0.037	0.057
K2O	0	0.024	0.02	0.032	0.005
P2O5	0.013	0.001	0	0	0
F	0.022	0	0.01	0.014	0
Cl	0	0	0.016	0.001	0
Total	95.943	91.358	96.634	96.601	93.458

O basis			3		
Si	0.000	0.003	0.003	0.002	0.011
Ti	3.875	0.852	4.034	3.886	1.989
Al	0.019	0.051	0.021	0.022	0.540
Cr	0.000	0.000	0.000	0.000	0.000
Fe3+	0.231	6.238	0.000	0.203	3.460
Fe2+	3.763	0.799	3.860	3.818	1.919
Mn	0.089	0.043	0.057	0.063	0.057
Mg	0.018	0.003	0.022	0.007	0.021
Ca	0.005	0.010	0.003	0.000	0.002
Zn	0.000	0.000	0.000	0.000	0.000
Ba	0.000	0.000	0.000	0.000	0.000
Na	0.002	0.001	0.002	0.004	0.006
K	0.000	0.002	0.001	0.002	0.000
P	0.001	0.000	0.000	0.000	0.001
Total	8.000	8.000	8.000	8.000	8.000
XMg	0.005	0.004	0.006	0.002	0.011
XFe3+	0.058	0.886	0.000	0.050	0.643
Fe3+/Fe2+	0.061	7.806	0.000	0.053	1.803

$X_{Mg} = Mg/[Mg+Fe^{2+})]$; $X_{Fe3+} = Fe^{3+}/[Fe^{2+}+Fe^{3+})]$;

Table 5.5: Representative chemical composition of pyroxene in mafic granulite (RNG 132B) sample

Analysis No.	2	3	7	10	29	33	34	12
SiO2	52.509	52.604	49.853	52.361	52.481	52.519	52.001	51.337
TiO2	0.104	0.035	0.57	0.159	0.135	0.099	0.289	0.059
Al2O3	1.269	1.129	4.078	1.026	1.338	1.011	1.717	0.461
Cr2O3	0.003	0	0.013	0.019	0	0.018	0	0
FeO	13.425	12.905	12.984	12.351	13.339	12.763	12.993	31.788
MnO	0.262	0.117	0.238	0.26	0.282	0.254	0.244	0.329
MgO	11.599	11.346	10.896	11.595	11.336	11.363	11.317	15.001
CaO	21.286	21.555	19.261	22.113	21.204	21.913	20.936	0.604
Na2O	0.383	0.383	0.848	0.262	0.487	0.094	0.477	0.039
K2O	0.009	0	0.317	0.009	0.008	0.008	0.127	0.018
P2O5	0.01	0.025	0.005	0.047	0.035	0.006	0.019	0
Total	100.859	100.099	99.063	100.202	100.645	100.048	100.12	99.636
O basis				6				
Si	1.974	1.992	1.898	1.981	1.978	1.995	1.968	2.015
Ti	0.003	0.001	0.016	0.005	0.004	0.003	0.008	0.002
Al	0.056	0.050	0.183	0.046	0.059	0.045	0.077	0.021
Cr	0.000	0.000	0.000	0.001	0.000	0.001	0.000	0.000
Fe3+	0.018	0.000	0.067	0.003	0.013	0.000	0.013	0.000
Fe2+	0.405	0.409	0.346	0.387	0.408	0.405	0.399	1.044
Mn	0.008	0.004	0.008	0.008	0.009	0.008	0.008	0.011
Mg	0.650	0.641	0.618	0.654	0.637	0.643	0.638	0.878
Ca	0.858	0.875	0.786	0.896	0.856	0.892	0.849	0.025
Na	0.028	0.028	0.063	0.019	0.036	0.007	0.035	0.003
K	0.000	0.000	0.015	0.000	0.000	0.000	0.006	0.001
Total	4.000	4.000	4.000	4.000	4.000	4.000	4.000	4.000
X_{Mg}	0.616	0.605	0.641	0.628	0.610	0.594	0.616	0.457
X_{Fe3+}	0.042	0.000	0.162	0.008	0.030	0.000	0.030	1.000

$X_{Mg} = Mg/[Mg+Fe^{2+})]$; $X_{Fe3+} = Fe^{3+}/[Fe^{2+}+Fe^{3+})]$;

Table 5.5: Representative chemical composition of garnet in mafic granulite (RNG 132B) sample

Analysis No.	1	4	15	17	19	30
SiO2	38.941	38.482	38.602	38.587	38.575	39.15
TiO2	0.022	0.033	0.05	0	0	0.055
Al2O3	22.087	22.164	21.771	21.737	21.972	22.195
Cr2O3	0.03	0	0	0.015	0	0.036
FeO	28.211	28.66	27.087	27.949	28.302	28.514
MnO	1.495	1.735	1.17	1.177	1.431	1.506
MgO	4.217	3.409	3.857	3.794	3.778	3.938
CaO	6.928	6.931	7.813	6.948	6.891	6.844
Na2O	0.016	0.023	0.004	0	0.023	0
K2O	0	0.006	0.003	0.002	0.015	0.016
P2O5	0.001	0	0.001	0.015	0	0
Total	101.948	101.443	100.358	100.224	100.987	102.254

O basis			12			
Si	3.008	3.001	3.026	3.036	3.015	3.020
Ti	0.001	0.002	0.003	0.000	0.000	0.003
Al	2.010	2.037	2.011	2.015	2.024	2.018
Cr	0.002	0.000	0.000	0.001	0.000	0.002
Fe3+	0.000	0.000	0.000	0.000	0.000	0.000
Fe2+	1.822	1.869	1.776	1.839	1.850	1.840
Mn	0.098	0.115	0.078	0.078	0.095	0.098
Mg	0.486	0.396	0.451	0.445	0.440	0.453
Ca	0.573	0.579	0.656	0.586	0.577	0.566
Total	8.000	8.000	8.000	8.000	8.000	8.000
X_{Mg}	0.210	0.175	0.202	0.195	0.192	0.198
Almandine	61.171	63.164	59.983	62.378	62.457	62.220
Spessartine	3.283	3.873	2.624	2.661	3.198	3.328
Pyrope	16.300	13.393	15.226	15.094	14.862	15.318
Grossular	19.229	19.571	22.167	19.858	19.483	19.113
Andradite	0.000	0.000	0.000	0.000	0.000	0.000
Uvarovite	0.018	0.000	0.000	0.009	0.000	0.021

$X_{Mg} = Mg/[Mg+Fe^{2+}]$; $X_{Fe3+} = Fe^{3+}/[Fe^{2+}+Fe^{3+}]$;

$X_{Alm} = Fe^{2+}/(Fe^{2+} + Mg + Mn + Ca)$; $X_{Prp} = Mg/(Fe^{2+} + Mg + Mn + Ca)$; $X_{Grs} = Ca/(Fe^{2+} + Mg + Mn + Ca)$.

$X_{Sps} = Mn/(Fe^{2+} + Mg + Mn + Ca)$.

Table 5.5: Representative chemical composition of hornblende in mafic granulite (RNG 132B) sample

Analysis No	9	11	13	21	24	25
SiO2	43.62	42.47	42.877	42.769	42.196	42.478
TiO2	2.064	2.138	2.546	2.299	2.394	2.23
Al2O3	11.363	12.311	12.081	11.812	12.334	11.573
Cr2O3	0	0.022	0	0.054	0.07	0.009
FeO	17.698	17.973	17.637	18.411	18.729	18.559
MnO	0.073	0.07	0.143	0.123	0.124	0.127
MgO	8.917	8.792	8.739	8.489	8.394	8.518
CaO	12.022	11.332	11.334	11.324	11.481	11.334
Na2O	2.044	2.009	2.1	2.073	2.13	2.033
K2O	1.279	1.431	1.454	1.391	1.516	1.439
P2O5	0.016	0	0	0	0	0.009
Total	99.096	98.548	98.911	98.745	99.368	98.309
O basis			23			
Si	6.503	6.361	6.406	6.419	6.315	6.411
Al iv	1.497	1.639	1.594	1.581	1.685	1.589
Al vi	0.500	0.534	0.533	0.508	0.490	0.470
Ti	0.231	0.241	0.286	0.260	0.269	0.253
Cr	0.000	0.003	0.000	0.006	0.008	0.001
Fe3+	0.000	0.128	0.000	0.036	0.059	0.073
Fe2+	2.207	2.123	2.204	2.275	2.285	2.270
Mn	0.009	0.009	0.018	0.016	0.016	0.016
Mg	1.982	1.963	1.946	1.899	1.873	1.917
Ca	1.920	1.818	1.814	1.821	1.841	1.833
Na	0.591	0.583	0.608	0.603	0.618	0.595
K	0.243	0.273	0.277	0.266	0.289	0.277
OH*	2.000	2.000	2.000	2.000	2.000	2.000
Total	17.684	17.675	17.687	17.690	17.748	17.705
X_{Mg}	0.473	0.480	0.469	0.455	0.450	0.458
X_{Fe3}	0.000	0.057	0.000	0.016	0.025	0.031

$X_{Mg}=Mg/[Mg+Fe^{2+}]$; $X_{Fe3+} = Fe^{3+}/[Fe^{2+}+Fe^{3+}]$;

Table 5.5: Representative chemical composition of biotite in mafic granulite (RNG 132B) sample

Analysis No.	16	18	20	27	28	32
SiO2	35.116	35.728	35.442	36.311	36.708	36.822
TiO2	5.121	4.746	5.062	4.894	5.09	5.326
Al2O3	14.127	14.384	14.769	14.53	14.893	14.792
Cr2O3	0	0.021	0.035	0	0	0.018
FeO	22.03	19.519	20.327	20.049	19.694	18.574
MnO	0.061	0.029	0	0.09	0.026	0.011
MgO	9.021	10.558	8.987	9.963	10.271	10.36
CaO	0.112	0.13	0.065	0.142	0.08	0.113
Na2O	0.137	0.315	0.187	0.018	0.094	0.054
K2O	9.797	9.643	9.834	9.468	9.706	8.866
P2O5	0.027	0.012	0.008	0.001	0	0
Total	95.549	95.085	94.716	95.466	96.562	94.936

O basis			22			
Si	5.466	5.507	5.508	5.564	5.548	5.601
Al iv	2.534	2.493	2.492	2.436	2.452	2.399
Al vi	0.058	0.120	0.213	0.188	0.200	0.252
Ti	0.599	0.550	0.592	0.564	0.579	0.609
Cr	0.000	0.003	0.004	0.000	0.000	0.002
Fe	2.868	2.516	2.642	2.569	2.489	2.363
Mn	0.008	0.004	0.000	0.012	0.003	0.001
Mg	2.093	2.426	2.082	2.276	2.314	2.349
Ca	0.019	0.021	0.011	0.023	0.013	0.018
Na	0.041	0.094	0.056	0.005	0.028	0.016
K	1.945	1.896	1.949	1.850	1.871	1.720
OH*	4.000	4.000	4.000	4.000	4.000	4.000
Total	19.632	19.630	19.549	19.488	19.497	19.331
X_{Mg}	0.578	0.509	0.559	0.530	0.518	0.501
Al total	2.592	2.613	2.705	2.624	2.653	2.652

$X_{Mg} = Mg/[Mg+Fe^{2+})]$; $X_{Fe3+} = Fe^{3+}/[Fe^{2+}+Fe^{3+})]$;

Table 5.5: Representative chemical composition of plagioclase in mafic granulite (RNG 132B) sample

Analysis No	6	14	23	26
SiO2	60.083	60.463	62.037	61.646
TiO2	0	0.001	0	0
Al2O3	26.378	26.492	26.283	26.041
Cr2O3	0	0.005	0.009	0
FeO	0	0.104	0.229	0.039
MnO	0	0	0	0.011
MgO	0.003	0	0	0.003
CaO	7.593	7.279	6.785	6.688
Na2O	6.943	7.591	8.342	8.398
K2O	0.265	0.267	0.282	0.237
P2O5	0.008	0.02	0.008	0.019
Total	101.273	102.222	103.975	103.082

O basis		8		
Si	2.643	2.640	2.664	2.668
Al	1.368	1.363	1.330	1.328
Ti	0.000	0.000	0.000	0.000
Fe	0.000	0.004	0.008	0.001
Mn	0.000	0.000	0.000	0.000
Mg	0.000	0.000	0.000	0.000
Ca	0.358	0.341	0.312	0.310
Na	0.592	0.643	0.695	0.705
K	0.015	0.015	0.015	0.013
P	0.000	0.001	0.000	0.001
Total	4.976	5.006	5.025	5.026
XOr	0.015	0.015	0.015	0.013
XAb	0.614	0.644	0.679	0.686
XAn	0.371	0.341	0.305	0.302

$X_{An} = Ca/(Ca+Na+K)$; $X_{Ab} = Na/(Ca+Na+K)$; $X_{Or} = K/(Ca+Na+K)$

Table 5.5: Representative chemical composition of ilmenite in mafic granulite (RNG 132B) sample

Analysis No	5	8	22	31
SiO2	0.051	0.056	0.094	0.015
TiO2	52.409	50.785	51.775	54.624
Al2O3	0.025	0.019	0.004	0
Cr2O3	0	0.017	0	0.016
FeO	44.932	44.93	45.857	44.409
MnO	0.964	0.585	0.611	0.798
MgO	0	0.365	0.454	0.02
CaO	0.103	0.485	0.66	0
Na2O	0.023	0	0	0.015
K2O	0.012	0.02	0	0.058
P2O5	0	0	0	0.034
Total	98.519	97.262	99.455	99.989
O basis		**3**		
Si	0.005	0.006	0.009	0.002
Ti	4.042	3.946	3.929	4.162
Al	0.003	0.002	0.000	0.000
Cr	0.000	0.001	0.000	0.001
Fe3+	0.000	0.092	0.123	0.000
Fe2+	3.953	3.791	3.746	4.092
Mn	0.084	0.051	0.052	0.068
Mg	0.000	0.056	0.068	0.003
Ca	0.011	0.054	0.071	0.000
Na	0.002	0.000	0.000	0.001
K	0.001	0.001	0.000	0.004
P	0.000	0.000	0.000	0.001
Total	8.000	8.000	8.000	8.000
XMg	0.000	0.015	0.018	0.001
XFe3+	0.000	0.024	0.032	0.000
Fe3+/Fe2+	0.000	0.024	0.033	0.000

$X_{Mg}=Mg/[Mg+Fe^{2+})]$; $X_{Fe3+} = Fe^{3+}/[Fe^{2+}+Fe^{3+})]$;

Table 5.6: Representative chemical composition of pyroxene in mafic granulite (RNG 122) sample

Analysis No.	78	79	80	83	94	96
SiO2	51.253	51.696	51.584	52.222	50.607	50.194
TiO2	0.15	0.069	0.062	0.105	0.003	0.037
Al2O3	1.601	1.161	0.876	0.98	0.527	0.465
Cr2O3	0	0	0	0.001	0	0
FeO	14.632	13.799	14.081	13.314	34.545	34.463
MnO	0.161	0.167	0.121	0.109	0.301	0.314
MgO	10.022	10.535	10.315	10.864	13.913	13.33
CaO	21.803	21.4	21.973	22.406	0.694	0.654
Na2O	0.493	0.429	0.321	0.374	0.02	0.014
K2O	0.002	0.004	0	0	0	0.001
Total	100.117	99.26	99.333	100.375	100.61	99.472

O-basis			6			
Si	1.955	1.983	1.982	1.978	1.987	1.999
Ti	0.004	0.002	0.002	0.003	0.000	0.001
Al	0.072	0.052	0.040	0.044	0.024	0.022
Cr	0.000	0.000	0.000	0.000	0.000	0.000
Fe^{3+}	0.047	0.009	0.016	0.022	0.004	0.000
Fe^{2+}	0.420	0.433	0.437	0.400	1.130	1.148
Mn	0.005	0.005	0.004	0.003	0.010	0.011
Mg	0.570	0.602	0.591	0.613	0.814	0.791
Ca	0.891	0.880	0.905	0.909	0.029	0.028
Na	0.036	0.032	0.024	0.027	0.002	0.001
K	0.000	0.000	0.000	0.000	0.000	0.000
Total	4.000	4.000	4.000	4.000	4.000	4.000
X_{Mg}	0.576	0.582	0.575	0.605	0.419	0.404
X_{Fe3+}	0.100	0.021	0.035	0.052	0.003	0.000

$X_{Mg} = Mg/[Mg+Fe^{2+})]$; $X_{Fe3+} = Fe^{3+}/[Fe^{2+}+Fe^{3+})]$;

Table 5.6: Representative chemical composition of garnet in mafic granulite (RNG 122) sample

Analysis No.	82	84	85	95
SiO2	38.011	38.087	38.121	38.347
TiO2	0.015	0	0.03	0.027
Al2O3	21.468	21.238	21.334	21.735
Cr2O3	0.008	0.013	0.026	0.015
FeO	30.151	29.667	30.084	30.363
MnO	0.939	0.953	1.022	0.876
MgO	2.869	2.817	2.944	2.758
CaO	7.456	7.316	7.398	7.331
Na2O	0.018	0	0.04	0.037
K2O	0	0.005	0	0.012
Total	100.935	100.096	100.999	101.501
O basis		12		
Si	2.993	3.023	3.000	3.005
Ti	0.001	0.000	0.002	0.002
Al	1.992	1.987	1.979	2.007
Cr	0.000	0.001	0.002	0.001
Fe3+	0.020	-0.034	0.015	-0.021
Fe2+	1.965	2.004	1.965	2.011
Mn	0.063	0.064	0.068	0.058
Mg	0.337	0.333	0.345	0.322
Ca	0.629	0.622	0.624	0.615
Total	8.000	8.000	8.000	8.000
X_{Mg}	0.146	0.143	0.150	0.138
X_{Fe3+}	0.010	-0.017	0.008	-0.011
Almandine	65.6	66.3	65.4	66.9
Spessartine	2.1	2.1	2.3	1.9
Pyrope	11.2	11.0	11.5	10.7
Grossular	20.8	20.9	20.6	20.7
Andradite	0.2	-0.4	0.2	-0.2
Uvarovite	0.0	0.0	0.0	0.0

X_{Mg} =Mg/[Mg+Fe^{2+})]; X_{Fe3+} = Fe^{3+}/[Fe^{2+}+Fe^{3+})];

X_{Alm}=Fe^{2+}/(Fe^{2+} + Mg+ Mn+ Ca); X_{Prp}= Mg/(Fe^{2+} +Mg + Mn+Ca); X_{Grs}= Ca/(Fe^{2+} +Mg +Mn +Ca).

X_{Sps}= Mn/(Fe^{2+} +Mg +Mn +Ca).

Table 5.6: Representative chemical composition of plagioclase in mafic granulite (RNG 122) sample

Analysis No.	77	81	87
SiO2	57.503	59.847	59.827
TiO2	0	0	0.001
Al2O3	26.159	25.252	24.925
Cr2O3	0	0.012	0
FeO	0.06	0.105	0.055
MnO	0	0	0.018
MgO	0.012	0	0.013
CaO	8.169	6.896	7.009
Na2O	6.821	7.68	7.537
K2O	0.228	0.106	0.138
Total	98.952	99.898	99.523

O-basis		8	
Si	2.601	2.670	2.678
Al	1.395	1.328	1.315
Ti	0.000	0.000	0.000
Fe	0.002	0.004	0.002
Mn	0.000	0.000	0.001
Mg	0.001	0.000	0.001
Ca	0.396	0.330	0.336
Na	0.598	0.664	0.654
K	0.013	0.006	0.008
Total	5.007	5.001	4.995
X_{Or}	0.013	0.006	0.008
X_{Ab}	0.594	0.664	0.655
X_{An}	0.393	0.330	0.337

$X_{An} = Ca/(Ca+Na+K)$; $X_{Ab} = Na/(Ca+Na+K)$; $X_{Or} = K/(Ca+Na+K)$

Table 5.6: Representative chemical composition of hornblende in mafic granulite (RNG 122) sample

Analysis No.	93	97	98
SiO2	41.861	41.339	40.891
TiO2	2.247	2.169	1.303
Al2O3	11.682	11.647	11.078
Cr2O3	0	0.03	0
FeO	20.028	20.412	21.325
MnO	0.075	0.082	0.055
MgO	7.563	7.613	7.901
CaO	11.489	11.446	11.525
Na2O	1.462	1.612	1.422
K2O	1.654	1.452	1.523
Total	98.061	97.802	97.023
O basis		23	
Si	6.372	6.309	6.284
Al iv	1.628	1.691	1.716
Al vi	0.467	0.403	0.291
Ti	0.257	0.249	0.151
Cr	0.000	0.000	0.000
Fe3+	0.146	0.287	0.605
Fe2+	2.403	2.318	2.136
Mn	0.010	0.011	0.007
Mg	1.716	1.732	1.810
Ca	1.874	1.871	1.898
Na	0.431	0.477	0.424
K	0.321	0.283	0.299
OH*	2.000	2.000	2.000
Total	17.626	17.631	17.620
X_{Mg}	0.417	0.428	0.459
X_{Fe3+}	0.057	0.110	0.221
total Al	2.096	2.095	2.007

$X_{Mg} = Mg/[Mg+Fe^{2+})]$; $X_{Fe3+} = Fe^{3+}/[Fe^{2+}+Fe^{3+})]$;

Table 5.7: Representative chemical composition of garnet in calc-silicate granofels (RNG 278A) sample

Analysis No.	36	48	53	58
SiO2	36.804	36.727	36.857	37.046
TiO2	0.332	0.387	0.136	0.266
Al2O3	8.221	7.746	8.396	9.118
Cr2O3	0.055	0	0.032	0.009
FeO	20.03	20.36	19.36	19.973
MnO	0.563	0.493	0.461	0.525
MgO	0	0.066	0.042	0.049
CaO	31.989	31.88	31.895	31.431
Na2O	0.015	0.018	0.006	0.022
K2O	0	0	0	0
P2O5	0.006	0	0.033	0.026
Total	98.015	97.677	97.218	98.465

O basis		12		
Si	2.996	3.003	3.018	2.997
Ti	0.020	0.024	0.008	0.016
Al	0.789	0.746	0.810	0.869
Cr	0.004	0.000	0.002	0.001
Fe3+	1.176	1.200	1.135	1.104
Fe2+	0.187	0.192	0.191	0.247
Mn	0.039	0.034	0.032	0.036
Mg	0.000	0.008	0.005	0.006
Ca	2.790	2.793	2.798	2.724
Total	8.000	8.000	8.000	8.000
X_{Mg}	0.000	0.040	0.026	0.023
X_{Fe3+}	0.863	0.862	0.856	0.817
Almandine	6.21	6.33	6.31	8.19
Spessartine	1.29	1.13	1.06	1.19
Pyrope	0.00	0.27	0.17	0.20
Grossular	37.06	35.38	38.48	39.81
Andradite	55.27	56.90	53.89	50.58
Uvarovite	0.17	0.00	0.10	0.03

X_{Mg} =Mg/[Mg+Fe^{2+})]; X_{Fe3+} = Fe^{3+}/[Fe^{2+}+Fe^{3+})];

X_{Alm}=Fe^{2+}/(Fe^{2+} + Mg+ Mn+ Ca); X_{Prp}= Mg/(Fe^{2+} +Mg + Mn+Ca); X_{Grs}= Ca/(Fe^{2+} +Mg +Mn +Ca).

X_{Sps}= Mn/(Fe^{2+} +Mg +Mn +Ca).

Table 5.7: Representative chemical composition of feldspar in calc-silicate granofels (RNG 278A) sample

Analysis No.	39	41	50
SiO2	55.834	58.741	56.645
TiO2	0.003	0.028	0.053
Al2O3	28.554	27.198	28.041
Cr2O3	0.018	0	0.032
FeO	0.172	0.089	0.16
MnO	0	0	0
MgO	0.001	0	0
CaO	9.761	8.351	9.399
Na2O	6.377	6.976	6.497
K2O	0.14	0.185	0.127
P2O5	0.01	0	0.033
Total	100.87	101.568	100.987
O basis		**8**	
Si	2.495	2.589	2.523
Al	1.504	1.413	1.472
Ti	0.000	0.001	0.002
Fe	0.006	0.003	0.006
Mn	0.000	0.000	0.000
Mg	0.000	0.000	0.000
Ca	0.467	0.394	0.449
Na	0.553	0.596	0.561
K	0.008	0.010	0.007
P	0.000	0.000	0.001
Total	5.033	5.007	5.021
X_{Or}	0.01	0.01	0.01
X_{Ab}	0.54	0.60	0.55
X_{An}	0.45	0.39	0.44

$X_{An} = Ca/(Ca+Na+K)$; $X_{Ab} = Na/(Ca+Na+K)$; $X_{Or} = K/(Ca+Na+K)$

Table 5.7: Representative chemical composition of epidote in calc-silicate granofels (RNG 278A) sample

Analysis No.	35	40	43	45	47	51	52	54	55	56	57	59	60	61
SiO2	37.452	37.958	37.854	38.01	38.17	37.146	37.985	37.913	37.644	37.99	36.907	37.718	37.405	37.317
TiO2	0.149	0.163	0.147	0.131	0.144	0.052	0.103	0.134	0.021	0	0.044	0.174	0.004	0.092
Al2O3	23.909	23.988	24.087	24.086	24.432	22.97	23.788	24.054	23.465	23.999	22.726	23.971	23.295	23.304
Cr2O3	0	0.006	0	0	0	0	0.018	0	0.008	0	0	0	0.024	0
FeO	11.087	11.037	10.727	11.489	11.033	11.573	11.398	11.108	11.492	11.169	11.85	11.017	11.311	11.245
MnO	0.006	0.023	0.011	0	0.008	0	0	0	0	0.042	0	0.022	0.045	0.019
MgO	0	0.026	0	0.006	0.028	0.026	0	0.033	0	0.002	0.01	0.001	0.027	0
CaO	22.848	22.944	22.642	23.095	23.103	22.094	22.804	22.878	22.696	23.001	21.542	22.961	22.309	22.412
Na2O	0.009	0	0	0.009	0.009	0.016	0.043	0.005	0	0.017	0	0	0.001	0
K2O	0	0	0	0.005	0	0	0.007	0	0.005	0.009	0	0.006	0.008	0
P2O5	0.034	0	0.057	0.02	0	0	0.01	0.015	0.047	0.032	0.02	0.018	0.027	0
Total	95.494	96.145	95.525	96.851	96.927	93.877	96.156	96.14	95.378	96.261	93.099	95.888	94.456	94.389

O basis — 12.5

	35	40	43	45	47	51	52	54	55	56	57	59	60	61
Si	3.005	3.021	3.029	3.008	3.012	3.030	3.025	3.018	3.025	3.022	3.035	3.012	3.033	3.027
Ti	0.009	0.010	0.009	0.008	0.009	0.003	0.006	0.008	0.001	0.000	0.003	0.010	0.000	0.006
Al	2.261	2.250	2.271	2.246	2.272	2.209	2.233	2.256	2.223	2.250	2.202	2.256	2.226	2.228
Fe+3	0.744	0.735	0.718	0.760	0.728	0.790	0.759	0.739	0.772	0.743	0.815	0.736	0.767	0.763
Mn	0.000	0.002	0.001	0.000	0.001	0.000	0.000	0.000	0.000	0.003	0.000	0.001	0.003	0.001
Mg	0.000	0.003	0.000	0.001	0.003	0.003	0.000	0.004	0.000	0.000	0.001	0.000	0.003	0.000
Ca	1.964	1.957	1.941	1.958	1.953	1.931	1.946	1.951	1.954	1.961	1.898	1.965	1.938	1.948
Na	0.001	0.000	0.000	0.001	0.001	0.003	0.007	0.001	0.000	0.003	0.000	0.000	0.000	0.000
K	0.000	0.000	0.000	0.001	0.000	0.000	0.001	0.000	0.001	0.001	0.000	0.001	0.001	0.000
H	1.000	1.000	1.000	1.000	1.000	1.000	1.000	1.000	1.000	1.000	1.000	1.000	1.000	1.000
Total	8.984	8.977	8.968	8.982	8.980	8.969	8.976	8.977	8.976	8.983	8.954	8.982	8.971	8.972

Table 5.8: Representative chemical composition of hornblende in amphibolite (RNG 283) sample

Analysis No.	97	103	105	111	112	115	124	127	128	134	135	137	139
SiO_2	43.932	44.485	44.274	48.125	46.147	45.241	44.553	44.61	44.621	44.967	44.399	44.261	44.202
TiO_2	1.419	1.475	1.415	0.945	0.95	1.16	1.133	0.961	0.978	1.117	1.288	1.175	0.901
Al_2O_3	11.908	11.647	12.075	8.911	10.205	11.399	12.054	11.951	11.735	11.201	11.244	11.95	12.363
Cr_2O_3	0.003	0.03	0.001	0.002	0.027	0.036	0.038	0.015	0.056	0.017	0.01	0.009	0.07
FeO	14.848	14.283	15.457	13.938	14.897	14.734	15.693	15.101	14.696	15.309	15.006	15.465	15.656
MnO	0.032	0.103	0.011	0.141	0.08	0.073	0.022	0.082	0	0.059	0.124	0.054	0.102
MgO	10.712	11.168	10.976	12.861	11.605	11.155	10.555	10.768	10.836	10.87	11.014	10.737	10.487
CaO	11.607	11.715	11.349	11.818	11.398	11.975	12.025	11.95	11.999	11.794	12.018	11.729	11.87
Na_2O	1.714	1.717	1.724	1.284	1.404	1.574	1.559	1.617	1.495	1.432	1.504	1.627	1.46
K_2O	1.078	1.078	1.018	0.662	0.722	1.048	1.147	1.126	1.066	0.978	0.97	1.143	1.171
P_2O_5	0	0.013	0	0	0.02	0	0.004	0	0.021	0	0.094	0.018	0
Total	97.253	97.714	98.3	98.687	97.455	98.395	98.783	98.181	97.503	97.744	97.671	98.168	98.282

O basis							23						
Si	6.531	6.570	6.477	6.929	6.761	6.6388	6.5431	6.5766	6.6161	6.637	6.581	6.522	6.506
Al iv	1.469	1.430	1.523	1.071	1.239	1.3612	1.4569	1.4234	1.3839	1.363	1.419	1.478	1.494
Al vi	0.617	0.597	0.558	0.441	0.523	0.6103	0.6295	0.6531	0.6669	0.585	0.546	0.598	0.651
Ti	0.159	0.164	0.156	0.102	0.105	0.1280	0.1252	0.1066	0.1091	0.124	0.144	0.130	0.100
Cr	0.000	0.004	0.000	0.000	0.003	0.0042	0.0044	0.0017	0.0066	0.002	0.001	0.001	0.008
Fe^{3+}	0.139	0.100	0.417	0.298	0.392	0.0811	0.1297	0.1063	0.0485	0.204	0.152	0.236	0.255
Fe^{2+}	1.707	1.664	1.474	1.380	1.433	1.7271	1.7977	1.7554	1.7738	1.686	1.708	1.670	1.673
Mn	0.004	0.013	0.001	0.017	0.010	0.0091	0.0027	0.0102	0.0000	0.007	0.016	0.007	0.013
Mg	2.374	2.459	2.394	2.761	2.535	2.4403	2.3108	2.3665	2.3952	2.392	2.434	2.359	2.301
Ca	1.849	1.854	1.779	1.823	1.789	1.8827	1.8921	1.8875	1.9062	1.865	1.909	1.852	1.872
Na	0.494	0.492	0.489	0.358	0.399	0.4478	0.4439	0.4622	0.4298	0.410	0.432	0.465	0.417
K	0.204	0.203	0.190	0.122	0.135	0.1962	0.2149	0.2118	0.2016	0.184	0.183	0.215	0.220
OH*	2.000	2.000	2.000	2.000	2.000	2.0000	2.0000	2.0000	2.0000	2.000	2.000	2.000	2.000
Total	17.547	17.548	17.458	17.303	17.323	17.527	17.551	17.562	17.538	17.459	17.524	17.531	17.509

(Ca+Na) (B)	2.000	2.000	2.000	2.000	2.000	2.000	2.000	2.000	2.000	2.000	2.000	2.000	2.000
Na (B)	0.151	0.146	0.221	0.177	0.211	0.117	0.108	0.112	0.094	0.135	0.091	0.148	0.128
(Na+K) (A)	0.547	0.548	0.458	0.303	0.323	0.527	0.551	0.562	0.538	0.459	0.524	0.531	0.509
Mg/(Mg+Fe2)	0.582	0.596	0.619	0.667	0.639	0.586	0.562	0.574	0.575	0.587	0.588	0.585	0.579
Fe3/(Fe3+Alvi)	0.183	0.144	0.428	0.403	0.429	0.117	0.171	0.140	0.068	0.258	0.218	0.283	0.281
Total Al	2.086	2.027	2.082	1.512	1.762	1.971	2.086	2.077	2.051	1.948	1.964	2.075	2.145

$X_{Mg} = Mg/[Mg+Fe^{2+}]$; $X_{Fe3+} = Fe^{3+}/[Fe^{2+}+Fe^{3+}]$;

Table 5.8: Representative chemical composition of garnet in amphibolite (RNG 283) sample

Analysis No.	98	100	102	104	106	107	109	113	114	118	120	123	132	133	136	140	142
SiO2	39.008	39.031	39.021	39.091	38.909	38.969	38.416	39.104	38.865	38.663	38.627	38.872	38.613	38.577	38.661	38.954	38.687
TiO2	0.01	0.008	0	0.028	0	0	0.04	0.013	0.035	0	0	0.005	0.087	0.021	0.013	0.021	0.004
Al2O3	21.934	22.085	22.107	21.981	21.968	22.136	22.021	22.009	22.102	22.069	21.941	22.073	21.898	21.856	21.972	22.003	21.967
Cr2O3	0	0.027	0	0.021	0	0	0.025	0.025	0.02	0	0.038	0.025	0.022	0.035	0.012	0	0.035
FeO	26.491	27.47	27.144	27.118	27.079	26.895	27.759	26.097	26.45	27.711	25.822	26.864	26.956	26.512	26.594	26.594	26.708
MnO	1.231	1.705	1.551	1.703	1.313	1.319	0.932	0.989	1.234	1.53	1.287	1.261	1.241	1.201	1.254	1.28	1.146
MgO	3.392	3.895	3.823	3.851	3.701	3.674	3.795	3.714	3.681	3.804	3.113	3.247	3.408	3.232	3.465	3.345	3.327
CaO	9.572	7.855	8.248	8.241	8.652	8.723	8.503	9.509	8.517	7.36	9.489	9.725	9.262	9.609	9.563	9.671	9.667
Na2O	0	0	0.023	0	0.016	0.011	0.014	0.025	0.024	0.008	0	0.023	0	0	0	0.046	0.026
K2O	0.002	0.008	0.02	0.004	0	0.011	0	0	0.007	0	0	0.002	0	0.018	0.009	0	0
P2O5	0	0.017	0.019	0.021	0	0.005	0	0.014	0.006	0	0	0	0.016	0.014	0.013	0.001	0.019
Total	101.64	102.101	101.956	102.059	101.638	101.743	101.505	101.499	100.941	101.145	100.317	102.097	101.503	101.075	101.556	101.915	101.586
O basis											12						
Si	3.004	2.999	2.999	3.003	3.001	2.997	2.988	3.003	2.994	2.993	2.996	2.996	2.994	2.997	2.996	3.000	2.996
Ti	0.001	0.000	0.000	0.002	0.000	0.000	0.002	0.001	0.002	0.000	0.000	0.000	0.005	0.001	0.001	0.001	0.000
Al	1.991	2.000	2.002	1.990	1.997	2.006	2.018	1.992	2.007	2.014	2.006	2.005	2.001	2.001	2.007	1.997	2.005
Cr	0.000	0.002	0.000	0.001	0.000	0.000	0.002	0.002	0.001	0.000	0.002	0.002	0.001	0.002	0.001	0.000	0.002
Fe3+	0.000	0.000	0.000	0.000	0.000	0.000	0.000	0.000	0.000	0.000	0.000	0.000	0.000	0.000	0.000	0.000	0.000
Fe2+	1.745	1.796	1.781	1.774	1.775	1.771	1.780	1.732	1.790	1.843	1.763	1.738	1.754	1.745	1.720	1.736	1.735
Mn	0.080	0.111	0.101	0.111	0.086	0.086	0.061	0.064	0.081	0.100	0.085	0.082	0.081	0.079	0.082	0.084	0.075
Mg	0.389	0.446	0.438	0.441	0.426	0.421	0.440	0.425	0.423	0.439	0.360	0.373	0.394	0.374	0.400	0.384	0.384
Ca	0.790	0.647	0.679	0.678	0.715	0.719	0.709	0.782	0.703	0.611	0.789	0.803	0.769	0.800	0.794	0.798	0.802
Zn	0.000	0.000	0.000	0.000	0.000	0.000	0.000	0.000	0.000	0.000	0.000	0.000	0.000	0.000	0.000	0.000	0.000
Ba	0.000	0.000	0.000	0.000	0.000	0.000	0.000	0.000	0.000	0.000	0.000	0.000	0.000	0.000	0.000	0.000	0.000
Na	0.000	0.000	0.002	0.000	0.001	0.001	0.001	0.002	0.002	0.001	0.000	0.002	0.000	0.000	0.000	0.003	0.002
K	0.000	0.000	0.001	0.000	0.000	0.001	0.000	0.000	0.000	0.000	0.000	0.000	0.000	0.000	0.001	0.000	0.000
P	0.000	0.001	0.001	0.001	0.000	0.000	0.000	0.000	0.000	0.000	0.000	0.000	0.001	0.000	0.000	0.000	0.001
Total	8.000	8.000	8.000	8.000	8.000	8.000	8.000	8.000	8.000	8.000	8.000	8.000	8.000	8.000	8.000	8.000	8.000
X_{Mg}	0.182	0.199	0.197	0.199	0.193	0.192	0.198	0.197	0.191	0.192	0.170	0.177	0.183	0.177	0.189	0.181	0.181
X_{Fe3+}	0.000	0.000	0.000	0.000	0.000	0.000	0.000	0.000	0.000	0.000	0.000	0.000	0.000	0.000	0.000	0.000	0.000
Fe3+/Fe2+	0.000	0.000	0.000	0.000	0.000	0.000	0.000	0.000	0.000	0.000	0.000	0.000	0.000	0.000	0.000	0.000	0.000
X_{Py}	0.130	0.149	0.146	0.147	0.142	0.141	0.147	0.142	0.141	0.147	0.120	0.125	0.131	0.125	0.134	0.128	0.128
X_{Spr}	0.027	0.037	0.034	0.037	0.029	0.029	0.021	0.021	0.027	0.034	0.028	0.027	0.027	0.026	0.027	0.028	0.025
X_{Alm}	0.581	0.599	0.594	0.591	0.591	0.591	0.595	0.577	0.597	0.616	0.588	0.580	0.585	0.582	0.574	0.578	0.579
X_{Grs}	0.263	0.216	0.226	0.226	0.238	0.240	0.237	0.260	0.235	0.204	0.263	0.268	0.257	0.267	0.265	0.266	0.268

X_{Mg} =Mg/[Mg+Fe^{2+})]; X_{Fe3+} = Fe^{3+}/[Fe^{2+}+Fe^{3+})];

X_{Alm}=Fe^{2+}/(Fe^{2+} + Mg+ Mn+ Ca); X_{Prp}= Mg/(Fe^{2+} +Mg + Mn+Ca); X_{Grs}= Ca/(Fe^{2+} +Mg +Mn +Ca).

X_{Sps}= Mn/(Fe^{2+} +Mg +Mn +Ca).

Table 5.8: Representative chemical composition of feldspar in amphibolite (RNG 283) sample

Analysis No.	125	126	129
SiO2	57.996	58.855	57.937
TiO2	0	0.026	0
Al2O3	27.653	27.771	27.704
Cr2O3	0	0	0.018
FeO	0.128	0.09	0.058
MnO	0	0	0
MgO	0	0	0.021
CaO	8.952	8.893	9.001
Na2O	6.531	6.739	6.905
K2O	0.263	0.294	0.262
P2O5	0	0.004	0.017
Total	101.523	102.672	101.923
O basis		8	
Si	2.717	2.728	2.703
Ti	0.000	0.001	0.000
Al	1.527	1.517	1.523
Cr	0.000	0.000	0.001
Fe	0.002	0.002	0.001
Mn	0.000	0.000	0.000
Mg	0.000	0.000	0.001
Ca	0.449	0.442	0.450
Na	0.297	0.303	0.312
K	0.008	0.009	0.008
P	0.000	0.000	0.000
Total	5.000	5.000	5.000
X_{Ab}	0.393	0.402	0.406
X_{An}	0.596	0.586	0.584
X_{Or}	0.010	0.012	0.010

X_{Ab} = Ca/(Ca+Na+K); X_{Ab} = Na/(Ca+Na+K); X_{Or} = K/(Ca+Na+K)

Table 5.8: Representative chemical composition of clino-pyroxene in amphibolite (RNG 283) sample

Analysis No.	119	141
SiO2	52.957	52.618
TiO2	0	0.018
Al2O3	1.14	1.116
Cr2O3	0	0.003
FeO	9.817	9.984
MnO	0.059	0.116
MgO	12.346	12.563
CaO	23.547	23.507
Na2O	0.411	0.394
K2O	0	0
P2O5	0.049	0
Total	100.326	100.319
O basis	**6**	
Si	1.980	1.966
Ti	0.000	0.001
Al	0.050	0.049
Cr	0.000	0.000
Fe3+	0.020	0.047
Fe2+	0.287	0.265
Mn	0.002	0.004
Mg	0.688	0.700
Ca	0.943	0.941
Na	0.030	0.029
K	0.000	0.000
Total	4.000	4.000
X_{Mg}	0.706	0.725
X_{Fe3+}	0.065	0.151

$X_{Mg}=Mg/[Mg+Fe^{2+}]$; $X_{Fe3+} = Fe^{3+}/[Fe^{2+}+Fe^{3+}]$;

Table 5.8: Representative chemical composition of ilmenite in amphibolite (RNG 283) sample

Analysis No.	131
SiO2	0.01
TiO2	51.569
Al2O3	0.047
Cr2O3	0
FeO	46.308
MnO	0.215
MgO	0.403
CaO	0
Na2O	0.051
K2O	0
P2O5	0.006
Total	98.609
O basis	**3**
Si	0.001
Ti	3.959
Al	0.006
Cr	0.000
Fe3+	0.074
Fe2+	3.880
Mn	0.019
Mg	0.061
Ca	0.000
Na	0.005
K	0.000
P	0.000
Total	8.000
XMg	0.016
XFe3+	0.019
Fe3+/Fe2+	0.019

$X_{Mg} = Mg/[Mg+Fe^{2+})]$; $X_{Fe3+} = Fe^{3+}/[Fe^{2+}+Fe^{3+})]$;

Table 5.9: Representative chemical composition of clino-pyroxene in metagabbro (RNG 214) sample

Analysis No.	143	146	150	151	157	175	177
SiO2	49.907	50.736	49.843	49.503	50.154	50.912	51.233
TiO2	0.135	0.088	0.348	0.451	0.352	0.081	0.07
Al2O3	2.605	2.072	3.485	3.488	3.48	1.645	1.735
Cr2O3	0.05	0	0.054	0.131	0.203	0.014	0
FeO	10.475	10.221	10.433	10.182	10.588	10.737	10.778
MnO	0.199	0.297	0.201	0.17	0.255	0.259	0.22
MgO	11.64	11.864	11.376	11.352	11.364	11.767	11.618
CaO	20.503	20.431	20.594	20.363	20.67	20.667	20.621
Na2O	0.611	0.705	0.765	0.825	0.801	0.718	0.714
K2O	0	0.01	0.001	0.002	0.004	0.004	0.004
P2O5	0.001	0	0.037	0	0	0.005	0.032
Total	96.126	96.424	97.137	96.467	97.871	96.809	97.025
O basis				6			
Si	1.947	1.970	1.923	1.921	1.922	1.973	1.983
Ti	0.004	0.003	0.010	0.013	0.010	0.002	0.002
Al	0.120	0.095	0.158	0.160	0.157	0.075	0.079
Cr	0.002	0.000	0.002	0.004	0.006	0.000	0.000
Fe3+	0.024	0.013	0.030	0.030	0.033	0.027	0.004
Fe2+	0.318	0.319	0.306	0.301	0.306	0.321	0.345
Mn	0.007	0.010	0.007	0.006	0.008	0.009	0.007
Mg	0.677	0.687	0.654	0.657	0.649	0.680	0.670
Ca	0.857	0.850	0.851	0.847	0.849	0.858	0.855
Na	0.046	0.053	0.057	0.062	0.060	0.054	0.054
K	0.000	0.000	0.000	0.000	0.000	0.000	0.000
Total	4.000	4.000	4.000	4.000	4.000	4.000	4.000
X_{Mg}	0.680	0.683	0.681	0.686	0.679	0.680	0.660
X_{Fe3+}	0.070	0.039	0.090	0.090	0.097	0.079	0.012

$X_{Mg} = Mg/[Mg+Fe^{2+}]$; $X_{Fe3+} = Fe^{3+}/[Fe^{2+}+Fe^{3+}]$;

Table 5.9: Representative chemical composition of ortho-pyroxene in metagabbro (RNG 214) sample

Analysis No.	147	149	152	153	156	158	179
SiO2	50.168	49.942	49.46	49.888	49.786	50.508	50.384
TiO2	0.022	0.004	0.048	0.02	0.072	0.05	0
Al2O3	1.019	1.135	2.23	1.718	1.969	1.089	1.098
Cr2O3	0.027	0.018	0.083	0.043	0.079	0.003	0
FeO	26.682	26.436	25.719	27.376	27.662	27.088	27.38
MnO	0.661	0.727	0.593	0.674	0.712	0.632	0.645
MgO	16.796	16.651	15.402	16.656	16.34	17.278	17.102
CaO	0.6	0.588	3.03	0.605	0.578	0.576	0.504
Na2O	0.006	0	0	0.007	0.011	0.045	0.052
K2O	0	0	0	0.008	0	0.001	0
P2O5	0.004	0	0.003	0.016	0.027	0.004	0
Total	95.985	95.501	96.568	97.011	97.236	97.274	97.165

O basis				6			
Si	2.007	2.008	1.970	1.977	1.973	1.991	1.990
Ti	0.001	0.000	0.001	0.001	0.002	0.001	0.000
Al	0.048	0.054	0.105	0.080	0.092	0.051	0.051
Cr	0.001	0.001	0.003	0.001	0.002	0.000	0.000
Fe3+	0.000	0.000	0.000	0.000	0.000	0.000	0.000
Fe2+	0.893	0.889	0.857	0.907	0.917	0.893	0.905
Mn	0.022	0.025	0.020	0.023	0.024	0.021	0.022
Mg	1.002	0.998	0.915	0.984	0.965	1.015	1.007
Ca	0.026	0.025	0.129	0.026	0.025	0.024	0.021
Na	0.000	0.000	0.000	0.001	0.001	0.003	0.004
K	0.000	0.000	0.000	0.000	0.000	0.000	0.000
Total	4.000	4.000	4.000	4.000	4.000	4.000	4.000
X_{Mg}	0.529	0.529	0.516	0.520	0.513	0.532	0.527

$X_{Mg} = Mg/[Mg+Fe^{2+}]$; $X_{Fe3+} = Fe^{3+}/[Fe^{2+}+Fe^{3+}]$;

Table 5.9: Representative chemical composition of hornblende in metagabbro (RNG 214) sample

Analysis No.	144	154
SiO2	38.975	39.746
TiO2	2.332	3.289
Al2O3	13.111	13.889
Cr2O3	0	0.229
FeO	16.856	15.493
MnO	0.023	0.153
MgO	8.496	8.327
CaO	11.045	10.753
Na2O	2.365	3.543
K2O	1.877	0.433
P2O5	0.006	0.01
Total	95.086	95.865

O basis	23	
Si	6.107	6.094
Al iv	1.893	1.906
Al vi	0.529	0.605
Ti	0.275	0.379
Cr	0.000	0.028
Fe3+	0.012	0.000
Fe2+	2.197	1.987
Mn	0.003	0.020
Mg	1.985	1.903
Ca	1.854	1.767
Na	0.719	1.053
K	0.375	0.085
OH*	2.000	2.000
Total	17.948	17.826
X_{Mg}	0.47	0.49
X_{Fe3+}	0.01	0.00
total Al	2.421	2.510

$X_{Mg} = Mg/[Mg+Fe^{2+})]$; $X_{Fe3+} = Fe^{3+}/[Fe^{2+}+Fe^{3+})]$;

Table 5.9: Representative chemical composition of feldspar in metagabbro (RNG 214) sample

Analysis No.	148	159	160	161	162	163	164	165	166	167	168	169	173	174	176
SiO2	65.779	54.368	54.368	54.068	52.194	51.755	52.292	51.891	54.066	52.282	54.819	52.494	60.608	67.308	66.75
TiO2	0	0.033	0.033	0	0	0.018	0	0.027	0.023	0.043	0.02	0.016	0	0	0.026
Al2O3	19.851	28.724	28.724	29.567	30.706	30.378	30.032	30.271	29.395	29.935	29.022	30.269	26.711	20.213	19.902
Cr2O3	0.001	0	0	0	0.008	0	0	0.005	0.003	0.025	0	0.01	0	0	0
FeO	0.055	0.081	0.081	0.039	0.031	0.059	0.073	0.02	0.081	0	0.09	0.081	0.505	0.046	0
MnO	0	0.013	0.013	0	0.019	0	0	0.013	0	0	0	0.031	0.006	0	0
MgO	0.024	0	0	0.012	0	0.013	0.005	0	0	0.004	0.023	0.003	0.688	0.004	0
CaO	0.08	10.487	10.487	11.128	12.268	12.564	12.116	12.495	11.144	12.089	10.487	12.293	6.84	0.093	0.112
Na2O	0.278	5.578	5.578	5.239	4.675	4.546	4.317	4.557	5.37	5.005	5.741	4.646	5.958	1.033	1.148
K2O	10.629	0.173	0.173	0.182	0.113	0.117	0.164	0.142	0.17	0.131	0.135	0.164	0.3	9.979	9.697
P2O5	0	0	0	0	0.014	0	0.017	0.016	0.001	0	0.013	0.041	0.02	0	0.021
Total	96.697	99.457	99.457	100.235	100.028	99.45	99.016	99.437	100.253	99.514	100.35	100.048	101.636	98.676	97.656
O basis									8						
Si	3.027	2.562	2.466	2.436	2.366	2.362	2.390	2.368	2.437	2.384	2.464	2.381	2.377	3.412	3.027
Al	1.077	1.446	1.535	1.570	1.641	1.634	1.618	1.628	1.562	1.609	1.538	1.618	1.621	0.000	1.072
Ti	0.000	0.001	0.001	0.000	0.000	0.001	0.000	0.001	0.001	0.001	0.001	0.001	0.000	1.208	0.000
Fe	0.002	0.007	0.003	0.001	0.001	0.002	0.003	0.001	0.003	0.000	0.003	0.003	0.003	0.001	0.002
Mn	0.000	0.001	0.000	0.000	0.001	0.000	0.000	0.001	0.000	0.000	0.000	0.001	0.000	0.000	0.000
Mg	0.002	0.001	0.000	0.001	0.000	0.001	0.000	0.000	0.000	0.000	0.002	0.000	0.000	0.000	0.000
Ca	0.004	0.416	0.510	0.537	0.596	0.615	0.593	0.611	0.538	0.591	0.505	0.597	0.593	0.005	0.004
Na	0.025	0.551	0.491	0.458	0.411	0.402	0.383	0.403	0.469	0.443	0.500	0.409	0.427	0.051	0.090
K	0.624	0.009	0.010	0.010	0.007	0.007	0.010	0.008	0.010	0.008	0.008	0.009	0.009	0.323	0.573
P							0.001	0.001				0.040		0.000	
Total	4.759	4.994	5.016	5.013	5.022	5.024	4.997	5.022	5.021	5.035	5.020	5.018	5.030	5.000	4.768
X_{Or}	0.956	0.009	0.010	0.010	0.006	0.007	0.010	0.008	0.010	0.0073	0.0076	0.0093	0.0087	0.853	0.858
X_{Ab}	0.038	0.565	0.486	0.455	0.406	0.393	0.388	0.394	0.461	0.4252	0.4939	0.4024	0.415	0.134	0.135
X_{An}	0.006	0.426	0.504	0.534	0.588	0.600	0.602	0.598	0.529	0.5675	0.4985	0.5883	0.576	0.013	0.007

X_{An} = Ca/(Ca+Na+K); X_{Ab} = Na/(Ca+Na+K); X_{Or} = K/(Ca+Na+K)

Table 5.10: Representative chemical composition of clino-pyroxene in metadolerite (RNG 53D) sample

Analysis No.	65	86	89
SiO2	51.753	50.11	46.879
TiO2	0.353	0.393	1.726
Al2O3	1.983	3.276	7.706
Cr2O3	0.028	0	0.012
FeO	11.371	11.974	14.209
MnO	0.227	0.252	0.063
MgO	11.758	11.306	10.207
CaO	22.059	21.87	16.872
Na2O	0.528	0.669	1.121
K2O	0	0.142	1.221
P2O5	0.002	0	0.002
Total	100.062	99.992	100.018

O basis		6	
Si	1.948	1.886	1.765
Ti	0.010	0.011	0.049
Al	0.088	0.145	0.342
Cr	0.001	0.000	0.000
Fe3+	0.034	0.115	0.170
Fe2+	0.324	0.262	0.277
Mn	0.007	0.008	0.002
Mg	0.660	0.634	0.573
Ca	0.890	0.882	0.681
Na	0.039	0.049	0.082
K	0.000	0.007	0.059
Total	4.000	4.000	4.000
X_{Mg}	0.670	0.708	0.674
X_{Fe3+}	0.094	0.306	0.380

XMg =Mg/[Mg+Fe2+)]; XFe3+ = Fe3+/[Fe2++Fe3+)];

Table 5.10: Representative chemical composition of ortho-pyroxene in metadolerite (RNG 53D) sample

Analysis No.	66	77	79	83	85	88	91
SiO2	50.934	51.89	50.565	50.996	50.942	51.063	51.045
TiO2	0.031	0.125	0.089	0.077	0.067	0.018	0.042
Al2O3	0.873	5.156	0.886	0.82	0.898	0.854	0.884
Cr2O3	0.005	0.016	0	0.027	0.011	0.025	0.011
FeO	30.39	28.966	30.744	31.272	30.176	30.238	30.73
MnO	0.707	0.633	0.586	0.617	0.637	0.764	0.63
MgO	15.659	13.402	15.692	15.735	15.783	15.76	15.733
CaO	0.591	1.338	0.563	0.531	0.654	0.627	0.592
Na2O	0.009	0.648	0.017	0	0.018	0	0.009
K2O	0.006	0.022	0.004	0.01	0	0.002	0.004
P2O5	0.002	0.003	0.004	0.01	0	0	0.043
Total	99.207	102.199	99.15	100.095	99.186	99.351	99.723
O basis				6			
Si	1.997	1.967	1.985	1.985	1.996	1.998	1.993
Ti	0.001	0.004	0.003	0.002	0.002	0.001	0.001
Al	0.040	0.230	0.041	0.038	0.041	0.039	0.041
Cr	0.000	0.000	0.000	0.001	0.000	0.001	0.000
Fe3+	0.000	0.000	0.000	0.000	0.000	0.000	0.000
Fe2+	0.997	0.918	1.009	1.018	0.989	0.990	1.003
Mn	0.023	0.020	0.019	0.020	0.021	0.025	0.021
Mg	0.915	0.757	0.918	0.913	0.922	0.919	0.916
Ca	0.025	0.054	0.024	0.022	0.027	0.026	0.025
Na	0.001	0.048	0.001	0.000	0.001	0.000	0.001
K	0.000	0.001	0.000	0.000	0.000	0.000	0.000
Total	4.000	4.000	4.000	4.000	4.000	4.000	4.000
X_{Mg}	0.479	0.452	0.476	0.473	0.482	0.482	0.477

$X_{Mg} = Mg/[Mg+Fe2+)]$; $X_{Fe3+} = Fe3+/[Fe2++Fe3+)]$;

Table 5.10: Representative chemical composition of feldspar in metadolerite (RNG 53D) sample

Analysis No.	67	68	69	70	71	72	73	74
SiO2	58.496	57.118	56.494	56.049	55.156	55.582	55.226	56.007
TiO2	0.026	0.106	0.065	0.095	0.204	0.012	0.046	0.08
Al2O3	27.681	28.625	29.018	29.09	29.238	29.338	29.247	29.354
Cr2O3	0.02	0.043	0.013	0.003	0	0	0	0
FeO	0.321	0.429	0.285	0.545	0.636	0.19	0.257	0.364
MnO	0	0	0.002	0	0	0.002	0	0.017
MgO	0	0.017	0	0.046	0.203	0	0.006	0.02
CaO	8.706	9.759	10.433	10.499	10.995	10.951	11.086	10.758
Na2O	6.832	6.123	5.953	5.8	5.481	5.637	5.564	4.972
K2O	0.124	0.131	0.138	0.276	0.33	0.12	0.12	0.122
P2O5	0.029	0.023	0	0.013	0.01	0.019	0.011	0.03
Total	102.235	102.374	102.401	102.416	102.253	101.851	101.563	101.724

O basis				8				
Si	2.725	2.653	2.618	2.601	2.563	2.585	2.576	2.610
Ti	0.001	0.004	0.002	0.003	0.007	0.000	0.002	0.003
Al	1.520	1.567	1.585	1.591	1.601	1.608	1.608	1.612
Cr	0.001	0.002	0.000	0.000	0.000	0.000	0.000	0.000
Fe^{3+}	0.006	0.007	0.005	0.010	0.011	0.003	0.005	0.006
Mn	0.000	0.000	0.000	0.000	0.000	0.000	0.000	0.001
Mg	0.000	0.001	0.000	0.003	0.014	0.000	0.000	0.001
Ca	0.435	0.486	0.518	0.522	0.547	0.546	0.554	0.537
Zn	0.000	0.000	0.000	0.000	0.000	0.000	0.000	0.000
Ba	0.000	0.000	0.000	0.000	0.000	0.000	0.000	0.000
Na	0.309	0.276	0.267	0.261	0.247	0.254	0.252	0.225
K	0.004	0.004	0.004	0.008	0.010	0.004	0.004	0.004
P	0.001	0.000	0.000	0.000	0.000	0.000	0.000	0.001
Total	5.000	5.000	5.000	5.000	5.000	5.000	5.000	5.000
XAb	0.413	0.360	0.339	0.330	0.307	0.316	0.311	0.293
XAn	0.582	0.635	0.656	0.660	0.681	0.679	0.685	0.702
XOr	0.005	0.005	0.005	0.010	0.012	0.004	0.004	0.005

XAn = Ca/(Ca+Na+K); XAb = Na/(Ca+Na+K); XOr = K/(Ca+Na+K)

Table 5.10: Representative chemical composition of biotite in metadolerite (RNG 53D) sample

Analysis No.	64	81	95
SiO2	35.687	35.27	35.72
TiO2	6.947	6.706	6.303
Al2O3	14.827	14.756	14.593
Cr2O3	0.032	0	0.007
FeO	20.235	19.846	19.934
MnO	0.048	0	0.021
MgO	9.937	9.608	9.569
CaO	0	0.104	0.032
Na2O	0.047	0.031	0.109
K2O	10.013	9.627	10.082
P2O5	0.018	0.016	0.018
Total	97.791	95.964	96.388
O basis		**22**	
Si	5.367	5.392	5.448
Al iv	2.628	2.608	2.552
Al vi	0.000	0.050	0.071
Ti	0.786	0.771	0.723
Cr	0.004	0.000	0.001
Fe^{2+}	2.545	2.537	2.543
Mn	0.006	0.000	0.003
Mg	2.228	2.189	2.175
Ca	0.000	0.017	0.005
Na	0.014	0.009	0.032
K	1.921	1.877	1.961
OH*	4.000	4.000	4.000
F	0.000	0.000	0.000
Cl	0.000	0.000	0.000
Total	19.498	19.451	19.514
Al total	2.628	2.659	2.623
X_{Mg}	0.467	0.463	0.461

$X_{Mg} = Mg/[Mg+Fe^{2+})]$; $X_{Fe3+} = Fe3+/[Fe^{2+}+Fe^{3+})]$;

Table 5.10: Representative chemical composition of hornblende in metadolerite (RNG 53D) sample

Analysis No.	84	90
SiO2	39.81	41.684
TiO2	2.907	2.166
Al2O3	13.897	11.735
Cr2O3	0	0.009
FeO	18.388	19.758
MnO	0.055	0.221
MgO	7.793	8.734
CaO	11.504	10.134
Na2O	2.255	1.872
K2O	2.135	1.716
P2O5	0	0
Total	98.744	98.029
O basis	**23**	
Si	6.045	6.237
Al iv	1.955	1.763
Al vi	0.532	0.307
Ti	0.332	0.244
Cr	0.000	0.001
Fe3+	0.000	0.848
Fe2+	2.335	1.625
Mn	0.007	0.028
Mg	1.764	1.948
Ca	1.871	1.625
Na	0.664	0.543
K	0.414	0.328
OH*	2.000	2.000
Total	17.919	17.495
Mg/(Mg+Fe2)	0.430	0.545
X_{Fe3+}	0.000	0.343

$X_{Mg} = Mg/[Mg+Fe^{2+})]$; $X_{Fe3+} = Fe^{3+}/[Fe^{2+}+Fe^{3+})]$;

Table 5.10: Representative chemical composition of ilmenite in metadolerite (RNG 53D) sample

Analysis No.	62	82	94
SiO2	0.02	0.037	0.068
TiO2	53.013	51.233	49.989
Al2O3	0.009	0.032	0.04
Cr2O3	0.028	0	0.001
FeO	47.505	45.809	45.766
MnO	0.671	0.344	0.555
MgO	0.099	0.175	0.099
CaO	0.016	0.187	0.078
Na2O	0	0.024	0.05
K2O	0.039	0.117	0.039
P2O5	0.004	0	0.006
Total	101.404	97.958	96.691
O basis		3	
Si	0.002	0.004	0.007
Ti	3.968	3.969	3.922
Al	0.001	0.004	0.005
Cr	0.002	0.000	0.000
Fe3+	0.057	0.051	0.137
Fe2+	3.897	3.895	3.856
Mn	0.057	0.030	0.049
Mg	0.015	0.027	0.015
Ca	0.002	0.021	0.009
Na	0.000	0.002	0.005
K	0.002	0.008	0.003
P	0.000	0.000	0.000
Total	8.000	8.000	8.000
XMg	0.004	0.007	0.004
XFe3+	0.014	0.013	0.034
Fe3+/Fe2+	0.015	0.013	0.036

$X_{Mg}=Mg/[Mg+Fe^{2+}]$; $X_{Fe3+} = Fe^{3+}/[Fe^{2+}+Fe^{3+}]$;

Table 5.11: Summary of pressure-temperature estimates from the studied high grade rocks of the Central Gneissic Belt.

Sample No.	Rock type	Thermo/barometer used	Model	Assumed P/T	Result
RNG 122		Grt-Cpx thermometer	Ganguly (1979)	10 kbar	749-782°C
		GCPQ (Di- barometer)	Moecher et al. (1988)	782°C	9.5 kbar
		GCPQ (Hd- barometer)	Moecher et al. (1988)	782°C	13.2 kbar
		Al -in -Hbl barometer	Anderson and Smith (1995)	600°C	7.44 kbar
	Mafic Granulite	Grt-Cpx thermometer	Ganguly (1979)	10 kbar	796.5-845.7°C
		Grt-Bt thermometer	Dasgupta et al. (1991)	6.5 kbar	700-735.9°C
		Hbl-Pl thermometer	Holland and Blundy (1994)	8 kbar	617-623°C
RNG 132B		Silica-CaTs-Anorthite barometer	McCarthy and Patino Douce (1998)	846°C	10.91 kbar
		GCPQ (Di- barometer)	Moecher et al. (1988)	846°C	9.0 kbar
		GCPQ (Hd- barometer)	Moecher et al. (1988)	846°C	12.8 kbar
		Al -in -Hbl barometer	Anderson and Smith (1995)	620°C	7.54 kbar
RNG 146C		Hbl-Pl thermometer	Holland and Blundy (1994)	8.0 kbar	696°C
		Hbl-Pl barometry	Anderson and Smith (1995)		6.19 kbar & 684.9°C
	Hornblende Gneiss	Al -in -Hbl barometer	Anderson and Smith (1995)	690°C	5.93 kbar
		Grt-Bt thermometry	Dasgupta et al. (1991)	6.5 kbar	594-695°C
RNG 102C		Grt-Ilm thermometry	Pownceby et al. (1987)		594-673°C
		Al -in -Hbl barometer	Anderson and Smith (1995)	695°C	6.20 kbar
RNG 120A		Opx-Ilm thermometer	Bishop et al. (1980)	8.0 kbar	712-822.5°C
		Hbl-Pl thermometry	Holland and Blundy (1994)	8.0 kbar	677.3°C
	Charnockite	Al -in -Hbl barometer	Anderson and Smith (1995)	677°C	6.07 kbar
		Silica-CaTs-Anorthite barometer	McCarthy and Patino Douce (1998)	842°C	7.20 kbar
RNG 158		Al -in -Hbl barometer	Anderson and Smith (1995)	700°C	6.26 kbar
RNG 283		Hbl-Pl thermometry	Holland and Blundy (1994)	8.0 kbar	578-610°C
	Amphibolite	Al -in -Hbl barometer	Anderson and Smith (1995)	600°C	7.01 kbar
		Grt-Cpx thermometer	Ganguly (1979)	8.0 kbar	717.91°C
		GCPQ (Di- barometer)	Moecher et al. (1988)	600°C	6.5 kbar
RNG 214		Hbl-Pl thermometer	Holland and Blundy (1994)	8.0 kbar	763.8°C
	Metagabbro		Anderson and Smith (1995)	755°C	7.43 kbar
		Two pyroxene thermometer	Kretz (1992)		653-664°C
		Al -in -Hbl barometer	Anderson and Smith (1995)	763°C	6.89 kbar